Facies (2018) 64:1
https://doi.org/10.1007/s10347-017-0513-0

ORIGINAL ARTICLE

# Sedimentology and depositional sequences of a Kimmeridgian carbonate ramp system, Lower Saxony Basin, Northern Germany

**Fanfan Zuo[1] · Ulrich Heimhofer[1] · Stefan Huck[1] · Friedrich Wilhelm Luppold[2] · Oliver Wings[3,5] · Jochen Erbacher[4]**

Received: 27 June 2017 / Accepted: 7 October 2017 / Published online: 25 October 2017


**Abstract** Shallow-marine Kimmeridgian (Late Jurassic) deposits in the Lower Saxony Basin (LSB) composed of alternating limestone, marl and claystone attract great palaeontological interest due to their rich invertebrate and vertebrate assemblages. Unfortunately, the absence of open-marine marker fossils and numerous sedimentary gaps in combination with lateral facies changes hamper the precise stratigraphic correlation of these strata on both a local and global scale. Here, an integrated approach combining carbonate microfacies analysis, ostracod biostratigraphy and high-resolution sequence stratigraphy is applied to two Kimmeridgian sections (Langenberg and Bisperode, 60 km apart) in the southeastern LSB. High-resolution carbonate microfacies analysis enables the definition of 19 microfacies types and seven microfacies associations, which can be arranged into facies belts along a carbonate ramp. Vertical microfacies, bed thickness and diagnostic surfaces define stacking patterns that are interpreted as small-, medium- and large-scale sequences. The ostracod biostratigraphic framework established in this study provides the required stratigraphic control. Correlation of the two studied sections reveals a more proximal setting for Bisperode than Langenberg and an overall shallowing-up trend from mid-ramp to proximal inner ramp developed in both sections. Furthermore, the majority of the medium-scale sequence boundaries defined in this study can be found in similar biostratigraphic positions in other European basins. Synsedimentary tectonics combined with high sediment accumulation rates can be identified as important controlling factors for the distribution and composition of the Kimmeridgian deposits in the LSB based on detailed correlation on both a regional and super-regional scale.

**Keywords** Lower Saxony Basin · Kimmeridgian · Carbonate microfacies · Sequence stratigraphy · Ostracod biostratigraphy

## Introduction

Within the Late Jurassic, the Kimmeridgian stage (157.3–152.1 Ma, Gradstein and Ogg et al. 2012) is considered as a time of global warmth (Valdes and Sellwood 1992; Hallam 1993; Abbink et al. 2001; Sellwood and Valdes 2008). Seawater temperature estimates based on oxygen isotope composition of low-Mg calcite shells indicate warm ocean surface waters in subtropical latitudes (Riboulleau et al. 1998; Malchus and Steuber 2002; Lécuyer 2003; Martin et al. 2014; Nunn and Price 2010; Alberti et al. 2017). Moreover, this interval corresponds to a worldwide second-order transgression, spanning the Late Oxfordian to Late Kimmeridgian (Hardenbol et al. 1998; Hallam 2001; Colombié and Rameil 2007). During this period of sea-level highstand, large parts of

**Electronic supplementary material** The online version of this article (doi:10.1007/s10347-017-0513-0) contains supplementary material, which is available to authorized users.

✉ Fanfan Zuo
zuo@geowi.uni-hannover.de

[1] Institut für Geologie, Leibniz Universität Hannover, Callinstraße 30, 30167 Hannover, Germany

[2] Neuwarmbüchener Straße 10, 30916 Isernhagen, Germany

[3] Niedersächsischen Landesmuseums Hannover, Willy-Brandt-Allee 5, 30169 Hannover, Germany

[4] Bundesanstalt für Geowissenschaften und Rohstoffe, Stilleweg 2, 30655 Hannover, Germany

[5] Zentralmagazin Naturwissenschaftlicher Sammlungen, Martin-Luther-Universität Halle-Wittenberg, Domplatz 4, 06108 Halle (Saale), Germany

Europe were covered by shallow epicontinental seas, allowing the widespread deposition of subtropical shoal–water carbonates (Morgans-Bell et al. 2001; Reolid et al. 2005; Hesselbo et al. 2009; Pearce et al. 2010; Lathuilière et al. 2015). In the Lower Saxony Basin (LSB) of northern Germany, Kimmeridgian strata are represented by a succession of alternating limestone, marl and claystone, which were deposited in shallow-marine and brackish waters on a gently dipping carbonate ramp (Fischer 1991; Weiß 1995; Gramann et al. 1997; Baldermann et al. 2015). These deposits host well-preserved and diverse invertebrate and vertebrate assemblages including remains of fish, crocodilians, turtles, dinosaurs and even mammals (Mudroch and Thies 1996; Sander et al. 2006; Wings and Sander 2012; Carballido and Sander 2013; Jansen and Klein 2014; Marpmann et al. 2014; Lallensack et al. 2015; Gerke and Wings 2016; Martin et al. 2016). Of particular significance was the discovery and excavation of numerous specimens of the dwarf sauropod *Europasaurus holgeri* from the Langenberg quarry in 1998 (Sander et al. 2006).

However, previous sedimentary investigations of the Upper Jurassic shallow-water deposits in the LSB have focused predominantly on the Oxfordian limestones (Gramann et al. 1997; Helm and Schülke 1998, 2006; Helm et al. 2003; Betzler et al. 2007; Kästner et al. 2008, 2010; Cäsar 2012). In contrast, detailed stratigraphic and sedimentary analyses and correlations of the overlying Kimmeridgian strata are hampered by the difficult age assignment as a result of the notorious lack of open-marine marker fossils, the prevalence of sedimentary gaps and lateral facies changes induced by sea-level fluctuations and/or synsedimentary tectonics (Betz et al. 1987; Gramann et al. 1997; Petmecky et al. 1999; Kley et al. 2008). Various biostratigraphic methods have been investigated in order to provide a better stratigraphic age constraint for the Kimmeridgian deposits, including the rare occurrence of isolated ammonite specimens (Schweigert 1996, 1999) and selected vertebrate remains (e.g. fish teeth) (Karl et al. 2006; Thies et al. 2007; Diedrich 2009), as well as ostracods, foraminifera, charophytes, spores and pollen or dinoflagellates (Schudack 1994, 1993, 1996; Weiß 1995; Luppold 2003; Gramann et al. 1997). Unfortunately, most of these stratigraphic schemes suffer from facies-dependent limitations and provide conflicting results. Ostracod biostratigraphy, in contrast, has been found to be a suitable and useful biostratigraphic tool, especially with respect to the Kimmeridgian and Tithonian intervals under study (Schudack, 1994; Weiß 1995; Gramann et al. 1997). An ostracod biostratigraphic scheme has been established for the Upper Jurassic succession in northern Germany, which enables correlations of the Kimmeridgian strata in the LSB with the Boreal standard ammonite zonation of Hardenbol et al. (1998) (Schudack, 1994; Weiß 1995; Gramann et al. 1997).

The aim of this study is to develop a high-resolution sedimentary and sequence-stratigraphic framework for the Kimmeridgian deposits in the LSB which can be used for both regional and larger-scale regional correlation. Herein, an integrated approach combining carbonate microfacies, sequence stratigraphy and ostracod biostratigraphy is applied to two outcrop sections (Langenberg and Bisperode) located in the southeastern LSB. A sequence-stratigraphic framework is established based on the stratigraphic distribution of carbonate microfacies (MF) types and analysis of depositional environments. The sequence-stratigraphic correlation of the two studied sections, integrated with ostracod biostratigraphic constraints, provides a better understanding of the main factors controlling Kimmeridgian sedimentary evolution in the LSB. In addition, an attempt to compare this record to successions in other European basins is carried out using the integrated stratigraphic results of this study.

## Geological setting

The elongate east–west-trending LSB is located on the southern margin of the Central European Basin, with a length of ~ 300 km and a width of ~ 65 km. During Kimmeridgian times, the LSB was located within the Sub-Boreal province (Wierzbowski et al. 2016) and occupied a palaeolatitude of about ~ 35°N (van Hinsbergen et al. 2015), bordered by the Rhenish Massif to the south and the Ringkøbing-Fyn High to the north (Fig. 1a).

The evolution of the LSB started in the Permian, created by rifting and/or thermal subsidence (Senglaub et al. 2006). In the Late Jurassic, a shallow epicontinental carbonate ramp began to develop (Gramann et al. 1997). Differential subsidence due to synsedimentary rifting resulted in the development of graben and horst structures (Gramann et al. 1997). Consequently, the thickness of the deposits can vary by tens of metres over a short distance (Hoyer 1965). Stratigraphic sections located in the uplifted horst area may contain fewer small- and medium-scale cycles compared to the adjacent graben area (Kästner et al. 2008).

This study covers the uppermost part of the Korallenoolith Formation and the Lower to Middle Süntel Formation, exposed to the south of Hannover (Fig. 1b). The boundary between the two formations is diachronous, corresponding to the Oxfordian–Kimmeridgian boundary or Early Kimmeridgian (Schudack 1994; Weiß 1995; Gramann et al. 1997; Helm 2005). Reef-bearing carbonates and oolitic limestones of the Korallenoolith Formation are indicative of a shallow-marine subtropical environment with limited terrestrial influx (Betzler et al. 2007; Kästner et al. 2008, 2010; Cäsar 2012). The Early Kimmeridgian part of the Korallenoolith is also known as the *Humeralis-Schichten* in some areas, since it is partially characterized by mass occurrences of the brachiopod *Zeilleria humeralis* (Gramann and Luppold 1991; Hoyer 1965; Gramann et al. 1997). The Süntel

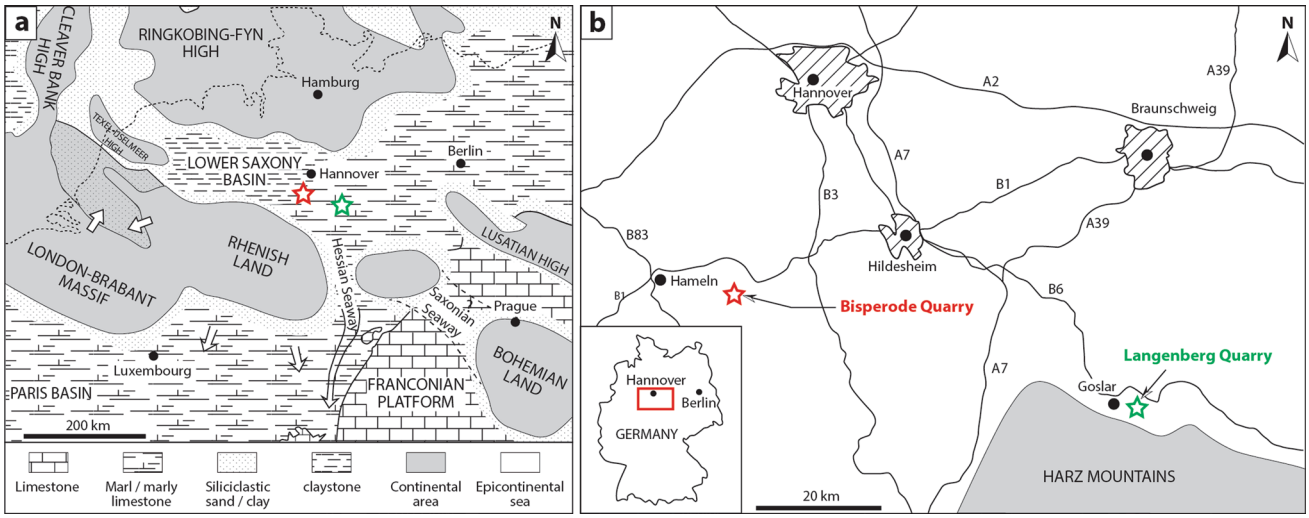


**Fig. 1** **a** Kimmeridgian palaeogeography and general facies distribution of the Lower Saxony Basin, northern Germany, and adjacent areas (combined and modified after Ziegler 1990 and Pieńkowski et al. 2008). **b** Location of the study area in northwest Germany with the two outcrops (Langenberg and Bisperode quarries) analysed in this paper

Formation, which is equivalent to the "Kimmeridge" in older literature (Hoyer 1965; Gramann et al. 1997; Schweigert 1999), is subdivided into the Lower, Middle and Upper Süntel Formations and covers early to late Kimmeridgian time. The depositional environment changed from open-marine platform carbonate towards a more shallow, lagoonal to peritidal setting characterized by strong salinity changes within this interval (Gramann et al. 1997; Mudroch et al. 1999).

A biostratigraphic division of the Upper Jurassic in northern Germany has been established based on ostracod assemblages (Schudack, 1994; Weiß 1995; Gramann et al. 1997). The Kimmeridgian strata in the LSB correspond to the interval between ostracod zones 7 and 15, and the boundary between the Oxfordian and Kimmeridgian stages is located at the base of zone 7. The uppermost Korallenoolith Formation assigned to the lowermost Kimmeridgian (*Humeralis-Schichten*) corresponds to zones 7 and 8. The Lower Süntel Formation covers the interval up to the top of zone 12, and the Middle and Upper Süntel Formations encompass zones 13 to 14 and zones 15 to 16, respectively (Fig. 2).

## Materials and methods

The Langenberg section (51°54′6.74″N, 10°30′27.73″E) is accessible in an active quarry about 5 km east of Goslar (Fig. 1b). The Bisperode section (52°04′00.09″N, 9°32′36.47″E), 60 km to the northwest, can be studied in an active quarry located about 2 km southwest of Lauenstein (Fig. 1b).

Both sections were logged and sampled bed-by-bed. A total of 443 samples (Langenberg: $n = 266$; Bisperode: $n = 177$) were collected in stratigraphic order, resulting in an average resolution of three samples per metre. The carbonate content of all samples was measured using a LECO CS230 carbon–sulphur analyser (LECO Corporation, Saint Joseph, MI, USA) after combustion of the samples in a high-frequency furnace at about 2000° C under an oxygen stream in the laboratories of the Federal Institute for Geosciences and Natural Resources (BGR). Macroscopic description of hand specimens was carried out, providing lithological and sedimentological information for the selection of samples for microfacies analysis. Carbonate microfacies analysis of 143 petrographic thin sections provides a semi-quantitative compilation of the main skeletal and non-skeletal grains (Flügel 2004) and of textural features. Classification follows Dunham (1962) and Embry and Klovan (1971). Facies belts and sedimentary models of Wilson (1975) and Flügel (2004) are used for interpretation of the depositional environment. The methodology and nomenclature proposed by Strasser et al. (1999) for shallow-water carbonates are used for sequence-stratigraphic interpretation. Following the approach of Kerans and Tinker (1997), facies proportion diagrams are established, which illustrate superimposed facies trends with stratigraphic height.

For ostracod taxonomy and biostratigraphy, 37 samples were collected from clay-rich horizons (Langenberg: $n = 25$; Bisperode: $n = 12$). Fresh samples (0.6–1.4 kg) were dried and soaked in hydrogen peroxide, disaggregated in water and subsequently washed through a 100-µm sieve. The residue was fractionated and quantitatively handled in a test sieve with a mesh width of 1.6 to 0.2 mm. The stratigraphic interpretation of the ostracod assemblages follows the schemes of Schudack (1994) and Weiß (1995) (Fig. 2).

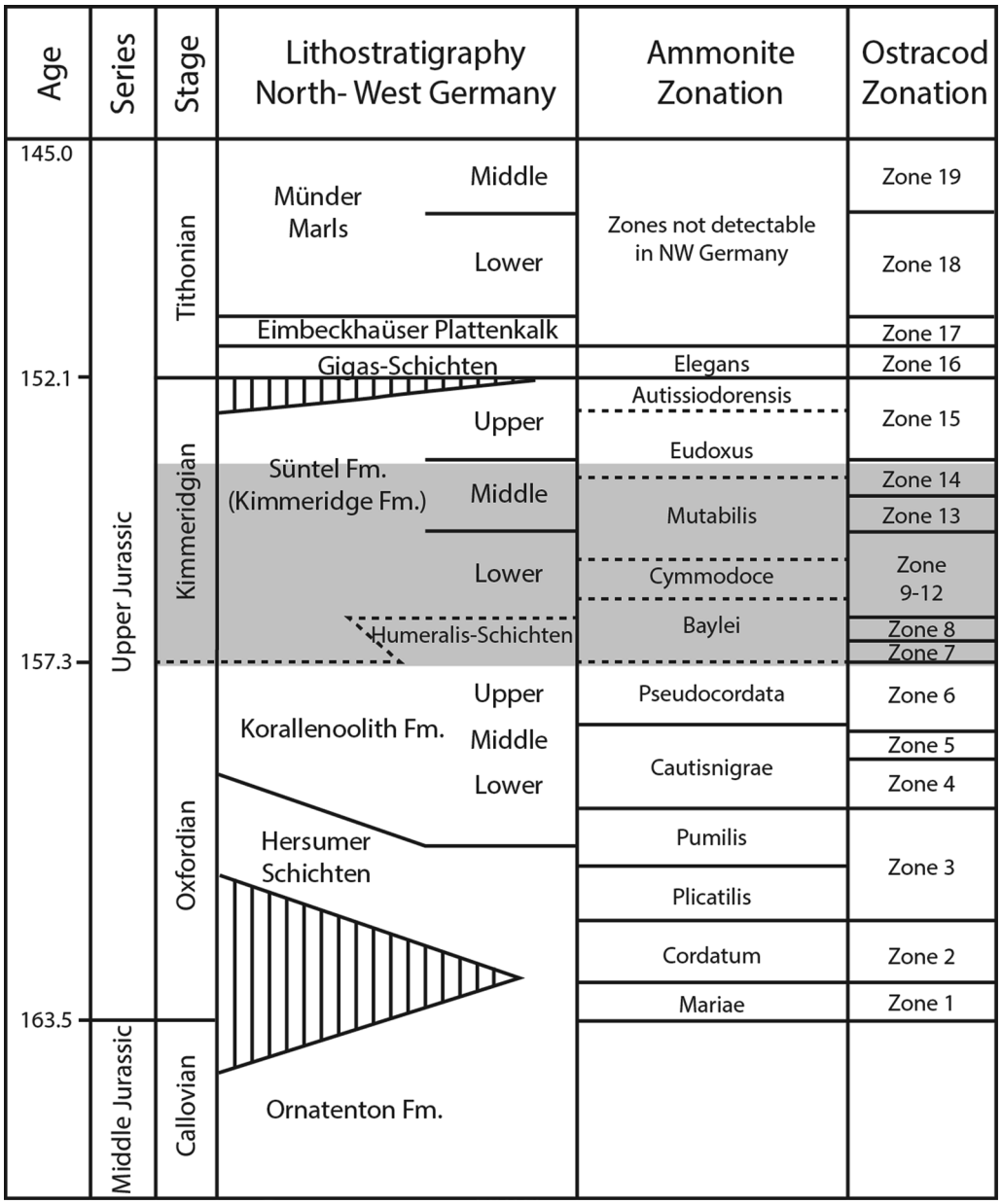


**Fig. 2** Lithostratigraphic scheme of the Late Jurassic in the Lower Saxony Basin, NW Germany, with the numerical age (Gradstein and Ogg 2012), as well as the standard zonation of the Boreal ammonite division (after Gramann et al. 1997) and ostracod zonation (after Schudack 1994; Weiß 1995)

## Results and interpretation

### Lithostratigraphy

*Langenberg section*

The Langenberg quarry provides a well-exposed section of Upper Jurassic shallow-marine deposits covering ~ 180 m, which was overturned due to tectonic uplift along the Harz boundary fault and now dips at an angle of 50–70° towards the south (Fig. 3a). Here, only the Kimmeridgian interval (uppermost 82.5 m) was investigated, which corresponds to bed numbers 24–154 in Fischer (1991) (Figs. 4 and 5).

The *Humeralis-Schichten* (0.0–21.0 m) represent a heterolithic unit composed of dark-brown sandy dolomite containing abundant shell debris with intercalated marl (0.0–5.3 m), thick-bedded oolitic limestone (5.3–12.0 m) and thin-bedded, dark-grey bioclastic limestone alternating with fossiliferous marl (12.0–21.0 m) (Fig. 5). Black-stained ooids and intraclasts (diameter < 2 mm) appear in the interval overlying the oolitic limestones. Upper bedding surfaces of oolitic and bioclastic limestones show signs of firm/hardground

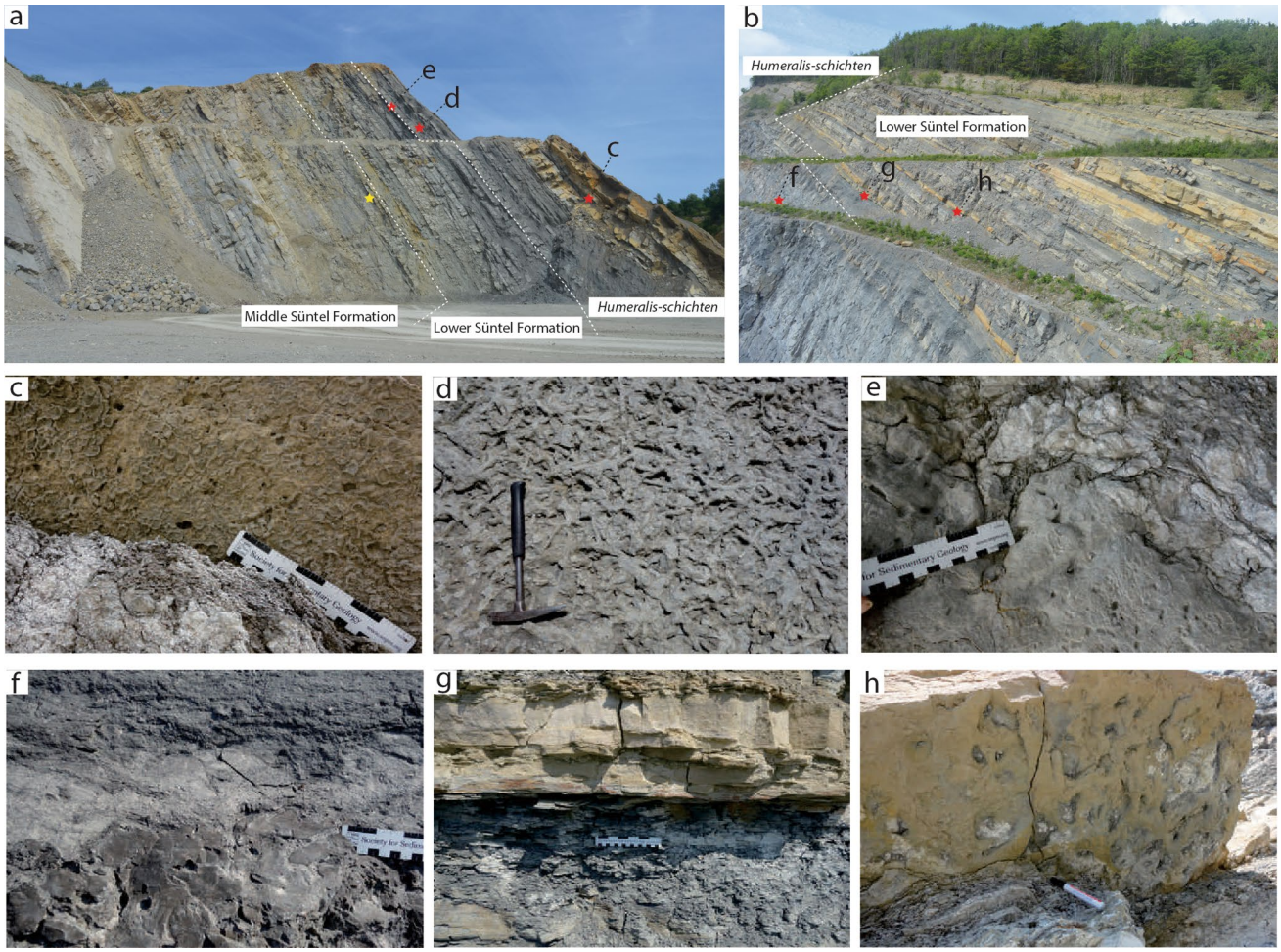


**Fig. 3** Field view and sedimentary characteristics of the exposed Kimmeridgian successions at the Langenberg and Bisperode quarry. **a** General view of the Langenberg section with the mark of strata showing images c, d and e (red star) as well as strata where the dinosaur (*Europasaurus holgeri*) was discovered (yellow star); **b** general view of the Bisperode section with the location of images f, g and h (red star); **c** hardground with abundant oysters attached, 8.5 m in the Langenberg section; **d** *Thalassinoides* bioturbation, 18.9 m in the Langenberg section; **e** hardground with borings and oysters attached, 20 m in the Langenberg section; **f** hardground with wave surface and borings, 1.5 m in the Bisperode section; **g** transition from shale to sandstone, 16–16.5 m in the Bisperode section; **h** *Thalassinoides* bioturbation, 23.3 m in the Bisperode section

formation with colonization by oysters (Fig. 3c) and vertical borings (Fig. 3e). Intense bioturbation is indicated by the dense meshwork of *Thalassinoides* burrows (Fig. 3d). Above, the Lower Süntel Formation (21.0–36.5 m) is composed of well-bedded, grey bioclastic limestone with dark argillaceous interbeds (21.0–32.7 m) passing up-section into greenish sandy limestone (32.7–33.8 m) and greenish dolomitic limestone (33.8–36.5 m). The overlying Middle Süntel Formation (36.5–82.5 m) is dominated by well-bedded micritic limestone containing no or rare bioclastic material. The middle interval (54.2–66.4 m) is composed of fine-grained pale-grey limestone showing a distinct nodular appearance. Rare float- to rudstone layers comprising gastropod accumulations occur in the uppermost part (63.4–66.4 m). Between 66.4 and 68.8 m, a conspicuous dark-brown dolomitic bed occurs ("Wasserbank" of Fischer 1991). Above, six conglomeratic layers are exposed (70.7–80.2 m), varying between 0.1 m and 1.4 m in thickness. Scattered sub-angular to sub-rounded clasts (size: 1–20 mm) occur embedded in a fine-grained micritic matrix (73.7–77.9 m) or form a dense, clast-supported fabric (78.8–80.2 m). Intercalated pale, micritic limestone beds show abundant vertical tube-shaped structures interpreted as *Skolithos* burrows (76.9–78.8 m).

Overall, carbonate content is high and varies between 13 and 99% (Fig. 5). The highest carbonate content (84–99%) is associated with the fine-grained limestones in the Middle Süntel Formation, whereas fluctuating and overall lower carbonate content occurs in the limestone–marl alternations of the Upper *Humeralis-Schichten* and Lower Süntel Formation.

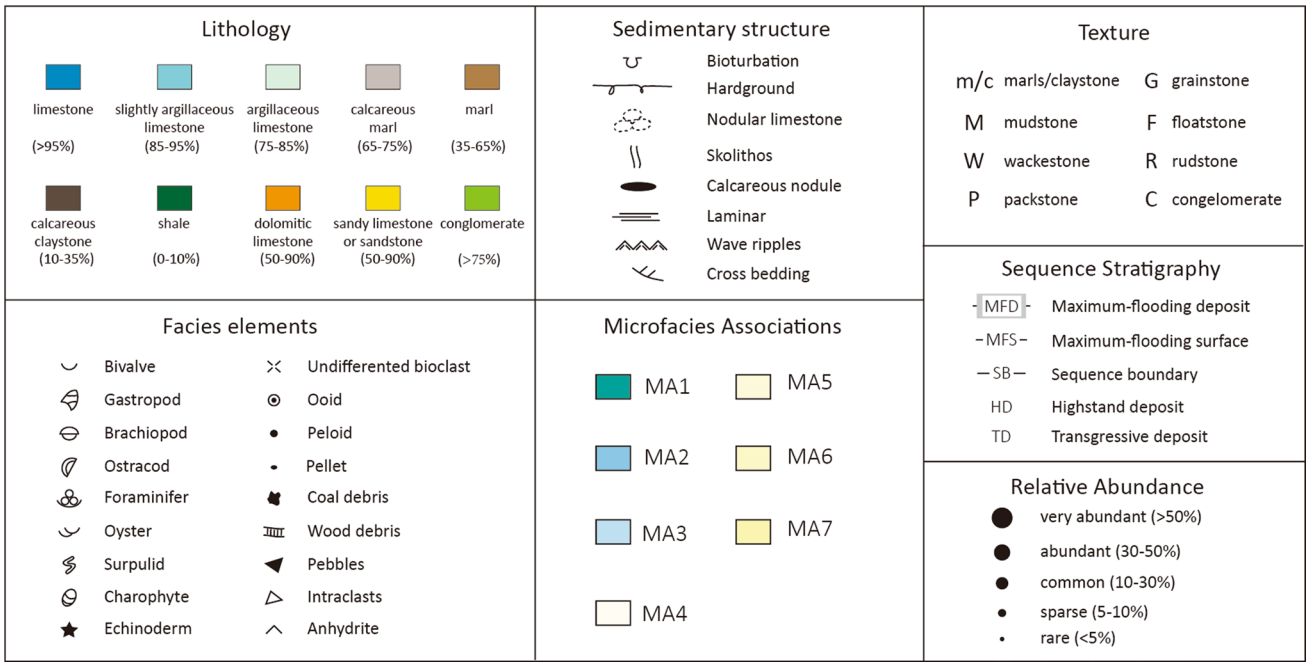


**Fig. 4** Legend for figures in this paper

*Bisperode section*

The active quarry comprising the Bisperode section exposes a ~ 160-m-thick succession covering the Korallenoolith and lowermost Süntel Formations. This study focuses on the uppermost part (55 m) constituted by the *Humeralis-Schichten* and Lower Süntel Formations (Fig. 3b).

The base of the studied section is composed of a 1.5-m-thick oolitic limestone (Figs. 4 and 6). This limestone is assigned to the Upper Korallenoolith Formation, which shows a well-developed hardground with an undulating surface and vertical, sediment-filled borings (Fig. 3f). The overlying *Humeralis-Schichten* (1.5–11.5 m) comprises mainly bioclastic limestone with marly interbeds, containing fragments of oysters, *Trichites*, serpulids and minor brachiopods. Above, the Lower Süntel Formation (11.5–54.3 m) is dominated by thick-bedded bioclastic and micritic limestone intercalated with sandy and clayish intervals. A dark-grey shale (13.0–16.2 m) with intercalated centimetre-thin sand layers occurs in the lower part, which is capped by a conspicuous, ochreous, fine-grained sandstone showing well-developed wave ripples and convolute bedding. The middle interval (16.9–43.2 m) is composed of alternations of bioclastic and micritic limestone separated by marly interbeds. Oysters, *Trichites* and rare brachiopods occur within several fossiliferous floatstone layers, some of which show well-developed *Thalassinoides* burrows (Fig. 3h). At 35.0 m and between 36.5 and 39.5 m, massive oolitic limestone with well-developed cross-bedding occurs. Up-section, the remaining part of the Lower Süntel Formation (43.2–54.3 m) is composed of fine-grained marl and claystone with intercalations of thin-bedded bioclastic and partly sandy limestone. The lowermost interval (43.2–49.6 m) is separated by a thin-bedded, yellowish limestone layer and shows conspicuous rhythmic changes in colour. Above, this interval is capped by a package of sandy and oyster-bearing limestone (49.6–51.1 m), which is overlain by an alternation of thick-bedded marl and thin-bedded micritic limestone (51.1–54.3 m).

The carbonate content shows significant variation, ranging between 2 and 96% (Fig. 6). Low carbonate content (< 50%) marks the clay-rich intervals (13.1–17.2 m; 43.2–54.2 m). The highest carbonate content occurs in the oolitic facies at the very base, and the thickest interval around 38 m.

*Biostratigraphy*

Conventional stratigraphic marker fossils (e.g. ammonites) are rare in the Upper Jurassic formations of the LSB due to the shallow and restricted nature of the deposits (Fischer 1991; Gramann et al. 1997). Instead, age assignment is based on ostracod assemblages in this study. Based on the ostracod zonation of Schudack (1994) and Weiß (1995), zones 6 to 14 are recognized in the two sections, encompassing the *Humeralis-Schichten* and the Lower and Middle Süntel Formations (Figs. 5 and 6). The ostracod biostratigraphy of the Langenberg section is based on new data (this study). For

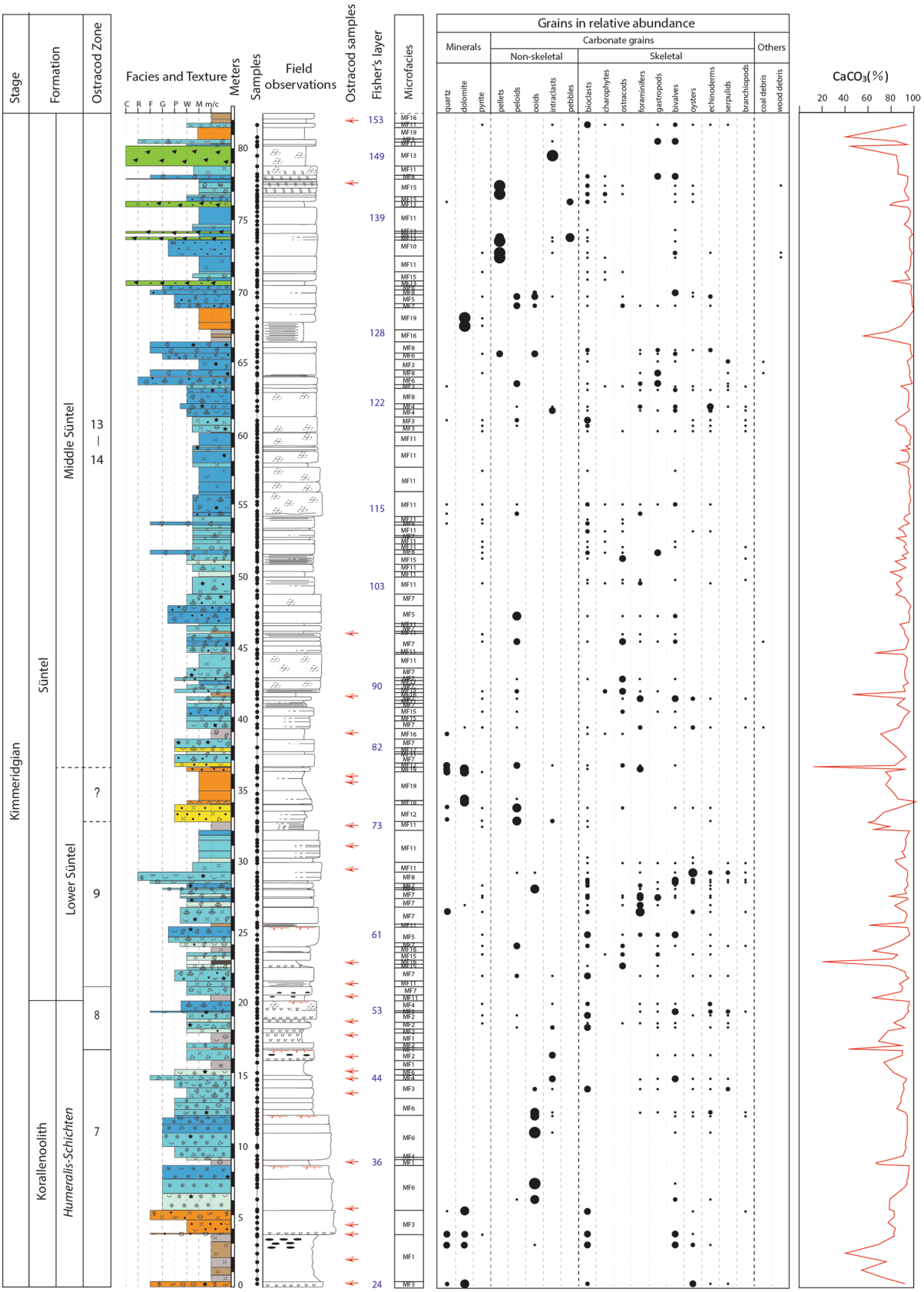


**Fig. 5** Integrated log of the Langenberg quarry showing lithology, texture, microfacies types and semi-quantitative results of component analysis and carbonate content, as well as the correlation with the bed numbering in Fischer (1991)

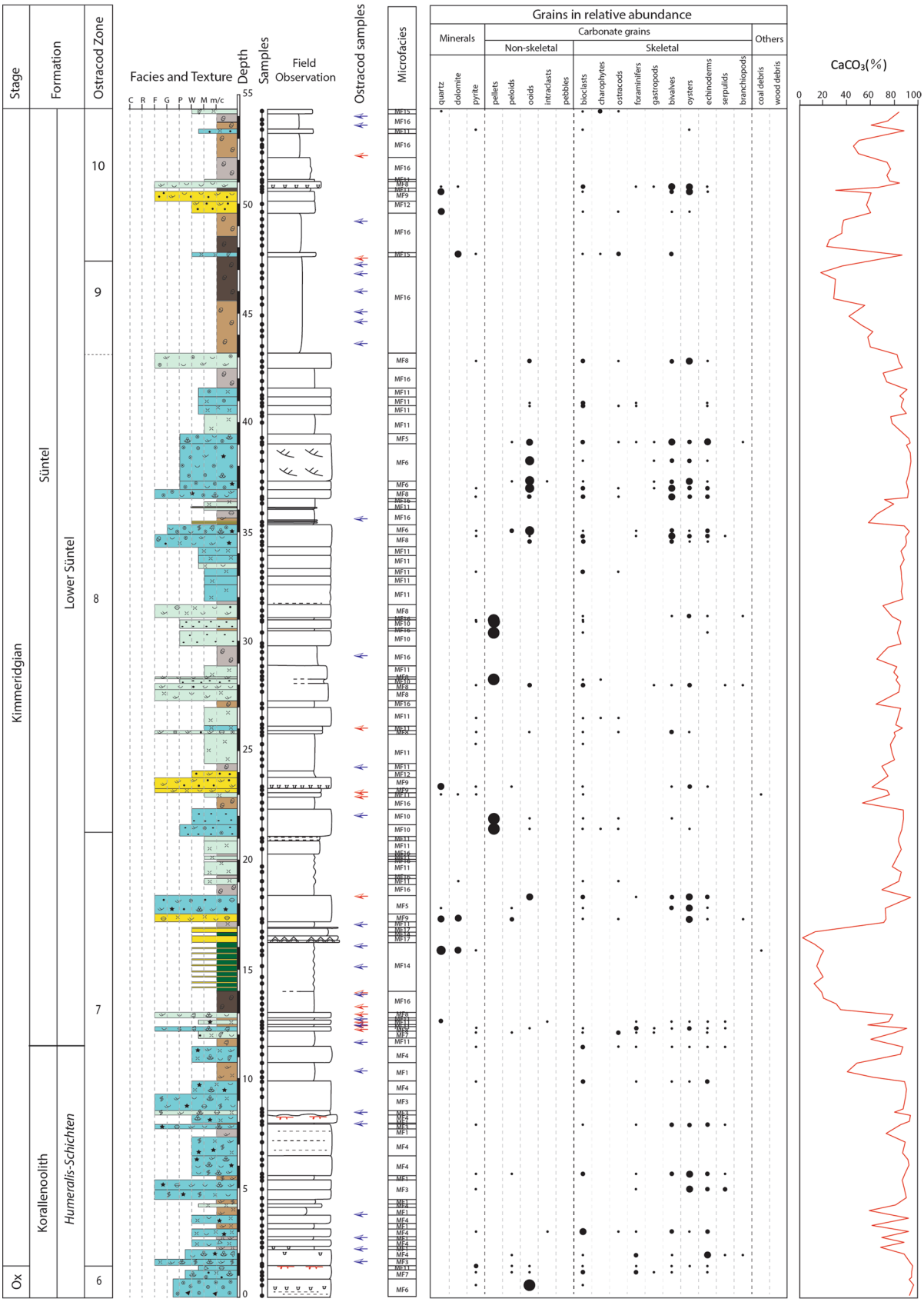
Stage
Formation
Ostracod Zone
Facies and Texture
Depth
Samples
Field Observation
Ostracod samples
Microfacies
Grains in relative abundance
Minerals
Carbonate grains
Non-skeletal
Skeletal
Others
quartz
dolomite
pyrite
pellets
peloids
ooids
intraclasts
pebbles
bioclasts
charophytes
ostracods
foraminifers
gastropods
bivalves
oysters
echinoderms
serpulids
branchiopods
coal debris
wood debris
CaCO3(%)
Kimmeridgian
Ox
Korallenoolith
Humeralis-Schichten
Lower Süntel
Süntel
10
9
8
7
6
C R F G P W M m/c

◂**Fig. 6** Integrated log of the Bisperode quarry showing lithology, texture, microfacies types and semi-quantitative results of component analysis and carbonate content. Ostracod samples from the present study are marked with red arrows, and those from the work of Weiß (1995) with blue arrows

the Bisperode section, it refers mainly to the results of Weiß (1995), with 11 additional new samples from this study.

Zone 6 is only constrained to the lowermost 1.5 m of the Bisperode section (Weiß 1995), which is characterized by only two species, *Galliaecytheridea dissimilis* and *G. mandelstami*, and assigned to the Late Oxfordian. Ostracod zones 7–8 are characterized by the species *Procytheropteron decoratum*, *Macrodentina pulchra*, *Paranotacythere interrupta* and *M. lineata*, indicative of the earliest Kimmeridgian. *Humeralis-Schichten* corresponds to zones 7 and 8 in the Langenberg section, but it is limited only in the lower part of zone 7 in the Bisperode section. Zone 8 is much more expanded in the Bisperode section (21.2–43.2 m) than in the Langenberg section (16.7–21.0 m). The Süntel Formation is constrained by the ostracod genus *Macrodentina*, which is adapted to both marine and brackish waters (Weiß 1995). Ostracod zones 9 to 12, corresponding to the Lower Süntel Formation, are characterized by the following taxa: *M. intercostulata*, *M. pulchra* and *M. lineata.* The Bisperode section comprises only ostracod zones 9 and 10. Zones 11 and 12, which are stratigraphically higher, are not determined in this section. The boundary between zones 9 and 10 is adjusted from 48.5 m (Weiß 1995) to 47.3 m, since a new sample 47.6 m (Pr.12, ESM_2) from the present study is defined as zone 10. In the Langenberg section, ostracod zone 9 (21.0–32.7 m) is present in the Lower Süntel Formation, whereas ostracod zones 10 to 12 are lacking, probably due to erosion. The overlying ostracod zones 13 to 14 in the Langenberg section correspond to the Middle Süntel Formation, characterized by the ostracod species *M. wicheri*, *M. rudis*, *M. ornata* and *Rectocythere iuglandiformis*. The biostratigraphic boundary between the Lower and Middle Süntel Formations is constrained by findings of the species *M. steghausi*. Additional data for ostracod assemblages are given in supplementary material EMS_1 and EMS_2.

## Microfacies associations

In total, 19 MF types have been differentiated for the Langenberg and Bisperode sections combined. MF types are described in Table 1 and illustrated in Figs. 7 and 8. All MF types are attributed to seven microfacies associations (MAs) representative of characteristic depositional environments (facies belts) ranging from mid-ramp to back-ramp settings. These MAs are described below from distal to proximal and in relation to their depositional characteristics.

### *MA1: Mid-ramp depositional setting*

This facies belt is present in the lowermost part of ostracod zone 7 in Bisperode and in ostracod zones 7 to 8 in Langenberg (Figs. 5 and 6). MA1 shows a gradual shift into MA2. It comprises two MF types including thin-bedded marlstone with bioclasts (MF type 1) and wackestone with ramp-derived intra- and/or bioclasts (MF type 2) (Table 1; Fig. 7a), with MF type 2 being restricted to the Langenberg section.

Some intraclasts show truncated ooids along the edge (Fig. 7a), evidence of erosion of the intraclasts from a landward oolitic shoal, most probably during episodic storm events. Small bioclastic debris finely dispersed within the matrix indicates calm hydrodynamic conditions below the fair-weather wave base (FWWB). Combined with the dense meshwork of *Thalassinoides* burrows, MF type 2 indicates reworking and low sedimentation rates in a mid-ramp setting (Flügel 2004; Betzler et al. 2007). Accumulation of brachiopods and strong bioturbation in the marlstone matrix of MF type 1, integrated with the gradual contact relationship with MF type 2, indicate open-marine conditions adjacent to MF type 2 (Strasser et al. 1999; Kästner et al. 2008).

### *MA2: Distal inner-ramp depositional setting*

This facies belt is represented in the lower part of both sections (Figs. 5 and 6). MF types of MA2 include bioclastic wacke- to floatstone with brachiopods, oysters and serpulid debris (MF type 3) (Table 1; Fig. 7b), as well as bioclastic wacke- to packstone with abundant echinoderm fragments and other bioclastic material (MF type 4) (Table 1; Fig. 7c). This facies belt shows accumulations of skeletal debris (e.g. brachiopod and oyster shells), which result from episodic storm events. The dominant components in MF type 3 can also be found occasionally in MF type 4 and vice versa.

Both the overall high diversity of fossils and abundance of echinoderm fragments indicate a medium-energy, open-marine environment with normal salinity (Flügel 2004). Rare findings of fragmentary ammonites and remains of marine crocodilians in the Langenberg section (Fischer 1991) confirm its open-marine character. Serpulids encrusting oyster shells indicate a low- to moderate-energy environment with low sedimentation rates (e.g. Schmid 1996; Krajewski et al. 2016), which is in accordance with findings of authigenic glauconite (Betzler et al. 2007; Baldermann et al. 2012). MA2 is typically intercalating with shoal deposits, thus reflecting a shallow subtidal setting between shoal and FWWB on the distal inner ramp (equivalent to the offshoal facies belt of Cäsar 2012). Subsequent dolomitization of the matrix in the lowermost part of the Langenberg section (0–5.3 m) results in a dolomitic cement, which formed

**Table 1** Microfacies association and microfacies types in the present study

| Microfacies association (MA) | Microfacies (MF) | | Description | Depositional environment and interpretation |
|---|---|---|---|---|
| MA1: Mid-ramp depositional setting | 1 | Thin-bedded marlstone with bioclasts | A mixture of clay and calcium carbonate predominant, with loose or weakly solid structure. Rare fossils, such as brachiopods, indicating normal marine environment | Mid-ramp deposition |
| | 2 | Wackestone with ramp-derived intra- and/or bioclasts | Mainly rounded but poorly sorted intraclasts from inner ramp, debris of undifferentiated fossils, as well as rare foraminifera, echinoderms, branchiopods, serpulids, etc. Normally associated with trace fossils *Thalassinoides*. Sparse pyrite (Fig. 7a) | Resedimentation in low- to medium-energy open-marine environment between the fair-weather and the storm wave base |
| MA2: Distal inner-ramp depositional setting | 3 | Bioclastic wacke- to floatstone with brachiopods, oysters and serpulid debris | Large fragments of brachiopods and oysters embedded in micritic matrix containing fine bioclastic debris. Serpulids appear separately or as encrustation attached to oysters. Rare debris of bivalves, gastropods, echinoderms, foraminifera (Fig. 7a, b) | Deposited in the distal part of inner ramp, close to the fair-weather wave base, with moderate energy level |
| | 4 | Bioclastic wacke- to packstone with abundant echinoderm fragments and other bioclastic material | Echinoderms most abundant bioclasts. Diverse fossils such as foraminifera, serpulids, oysters, brachiopods and peloids/ooids also present. Fine bioclasts give lime mud matrix dirty appearance. Rare glauconite (Fig. 7a–c) | Shallow subtidal setting, with medium–high energy conditions, close to the sand shoal in the inner ramp |
| MA3: High-energy shoal depositional setting | 5 | Bioclastic pack- to grainstone with abundant fossil fragments | Common well-sorted and sub-rounded bioclasts consisting of bivalves, gastropods, echinoderms, foraminifera, etc., as well as well-sorted peloids and ooids. Both sparry calcite cements and micritic matrix appear (Fig. 7a–d) | Interpreted as sand shoal deposition in the inner ramp |
| | 6 | Oolitic pack- to grainstone | Abundant or very abundant well-sorted ooids (0.2–0.8 mm, with an average size of 0.5 mm). Rare or sparse fragments of bivalves, echinoderms, gastropods, branchiopods, etc. All the component was packed in sparry calcite cement (normally) or lime mud matrix (locally) (Fig. 7a–e) | Representing the highest-energy subtidal sand shoal deposition in the inner ramp |

**Table 1** (continued)

| Microfacies association (MA) | Microfacies (MF) | | Description | Depositional environment and interpretation |
|---|---|---|---|---|
| MA4: Semi-restricted lagoon depositional setting | 7 | Peloidal bioclastic wacke- to packstone with ostracods and foraminifera | Diverse bioclasts, dominated by micritized foraminifera, ostracods, bivalves, echinoderms, as well as peloids or ooids from the sand shoal, are loosely packed in pure and dark-grey micritic matrix. Peloids are rounded or irregularly shaped grains with micritic envelope and relict structure (Fig. 7a–f) | Moderate-energy intertidal deposition near the sand shoal on the landward side |
| | 8 | Bioclastic wacke- to floatstone with bivalves and gastropods | Recrystallized large bivalve or gastropod composed of sparry calcite floating in a dense lime mud matrix. Rare other kinds of bioclasts (Fig. 7a–g/h) | Shallow subtidal deposition in the transition zone between open-marine and restricted settings, with moderate water energy |
| | 9 | Sandy limestone with large mollusc fragments | Sandy limestone dominated by evenly distributed, sand-sized, sub-angular to sub-rounded quartz (15–30%) and large bivalve fragments (0.5-2 mm). The matrix are fine microspar and/or recrystallized dolomite (10–20%) (Fig. 7a–i) | The size and low diversity of shell fragments indicate a semi-restricted lagoon deposition influenced by terrestrial influx |

**Table 1** (continued)

| Microfacies association (MA) | | Microfacies (MF) | Description | Depositional environment and interpretation |
|---|---|---|---|---|
| MA5: Restricted lagoon depositional setting | a | 10 Pelletal pack- to grainstone | Abundant well-sorted and well-rounded pellets are packed intensely. Rare intraclasts and fragments of bivalves, echinoderms, ostracods and charophytes also appear. Some wood debris can also be observed in Langenberg section (Fig. 7b–a) | Restricted shallow subtidal setting near lagoon centre in low energy level |
| | | 11 Bioclastic mud- to wackestone | Dark lime mud containing rare fine shell fragments (< 5%), such as bivalves, gastropod, charophytes, ostracods, etc. (Fig. 7b) | Low-energy deposition in the restricted lagoon centre |
| | | 12 Peloidal sandy limestone | Sandy limestone dominated by peloids and rare to sparse fine skeletal particles, with sand-sized quartz (5–30%) evenly scattered among micritic matrix. Rare pyrite occurs (Fig. 7b–c) | Lagoon deposition influenced by certain terrestrial influx |
| | | 13 Limestone conglomerate | Common to abundant poorly sorted (0.5–10 mm) and subangular black pebbles composed of mudstone or pelletal packstone containing rare bioclasts such as charophytes, ostracods and bivalves. These pebbles are compacted or float in the matrix made of densely packed pellets. Rare undifferentiated bioclasts and fragments of bivalves (Fig. 7b–d) | Interpreted as debris flow deposition formed in the lagoon setting |
| | b | 14 Shale–claystone alternations with sandy interbeds | Thin-laminated (1–2 cm) dark claystone with rare debris. The carbonate content is less than 20% (Fig. 3g) | Lagoonal deposition formed during a sea-level fall with significant terrestrial supply. |
| MA6: Intertidal back-ramp depositional setting | a | 15 Mud- to wackestone with charophytes and ostracods | Mud- to wackestone with rare to sparse integrated charophytes and ostracods of ovoid or lensoid shape, which also appear separately in different layers. Minor foraminifera and undifferentiated shell debris occur. Accompanied by *Skolithos* in the upper part of the Langenberg section (Fig. 7b–e/f) | Restricted shallow subtidal or intertidal deposition, low- to medium-energy condition |
| | | 16 Charophyte-rich marl or claystone | A mixture of lime mud and clay (25–90%) with very rare charophytes (Fig. 7b–g) | Low-energy intertidal deposition in a restricted lagoon environment |
| | b | 17 Fine-grained sandstone | Pure, fine-grained sandstone only appears intercalated with shale–claystone alternations in the Bisperode section (13–17 m), showing small-scale wave ripple cross-lamination and convolution structure | Coastal sandy tidal-flat deposition influenced by sufficient terrestrial influx during a fall in relative sea level |

**Table 1** (continued)

| Microfacies association (MA) | Microfacies (MF) | | Description | Depositional environment and interpretation |
|---|---|---|---|---|
| MA7: Supratidal back-ramp depositional setting | 18 | Evaporite–dolomite couplets | Gypsum crystals are distributed in a layered structure within fine-grained dark dolomite. Only occurs in a single layer in the Langenberg section (Fig. 7b–h) | Sabkha environment in supratidal based on the appearance of both gypsum and dolomite |
| | 19 | Dolomitic mudstone | Mainly very fine dolomite rhombs (45–90%) with rare skeletal particles. Quartz normally accounts for about 5–15% of the rock. Fenestral and algae lamination structure can be observed (Fig. 7b–i) | Restricted supratidal environment |

at shallow burial depth by replacement (Baldermann et al. 2015).

*MA3: High-energy shoal depositional setting*

This association occurs in several intervals at both localities and comprises bioclastic pack- to grainstone with abundant fossil fragments (MF type 5) and oolitic pack- to grainstone (MF type 6) (Table 1; Figs. 5, 6 and 7d, e).

Ooids form in agitated waters influenced by waves and currents within shallow-marine subtropical waters above the FWWB (Tucker and Wright 1990; Flügel 2004; Betzler et al. 2007), which is further confirmed by the appearance of cross-bedding. Well-sorted bioclasts in high diversity and a pack- to grainstone texture further indicate moderate- to high-energy shallow-water conditions of a shoal setting for MF type 5 (Wilson 1975; Flügel 2004). Based on comparison with modern analogues (Hine 1977; Burchette et al. 1990; André et al. 2003), MA3 is interpreted to represent a submarine oolitic-bioclastic shoal in a storm- and/or tide-influenced subtidal setting, located next to MA2 (Betzler et al. 2007; Kästner et al. 2008; Cäsar 2012).

*MA4: Semi-restricted lagoon depositional setting*

MA4 is present in the middle and upper part of both sections and is typically overlain by MA5/6 (Figs. 5 and 6). MA4 incorporates three MF types (Table 1; Figs. 7f–i) including peloidal bioclastic wacke- to packstone with ostracods and foraminifera (MF type 7), bioclastic wacke- to floatstone with bivalves and gastropods (MF type 8), and sandy limestone with large mollusc fragments (MF type 9), the latter being restricted to a small number of thin horizons in the Bisperode section.

The presence of a low-diversity assemblage (e.g. miliolid foraminifera and ostracods) and sparse echinoderm fragments and ooids in MF type 7 reflects a moderate- to high-energy near-shoal environment (Flügel 2004; Colombié and Strasser 2005; Cäsar 2012). Randomly oriented recrystallized molluscan shell fragments embedded within a micritic matrix (MF type 8) indicate a semi-restricted lagoon setting with moderate hydrodynamic conditions (Wilson 1975; Flügel 2004). In addition, mass occurrences of gastropods or bivalves in MF type 8 point to episodic high nutrient supply, which could be induced by a restriction of the lagoon during relative sea level fall (Dauwalder and Remane 1979; Dupraz and Strasser 1999; Kästner et al. 2008; Cäsar 2012) or stratification during a sea-level rise. Finely dispersed angular quartz associated with large shell debris in MF type 9 suggests an upper subtidal setting under high-energy conditions with a certain terrestrial influx (Pettijohn et al. 1987; Wilson 1975; Bauer et al. 2002; Flügel 2004). The pseudo-spar matrix indicates formation of MF type 9 close to the coast.

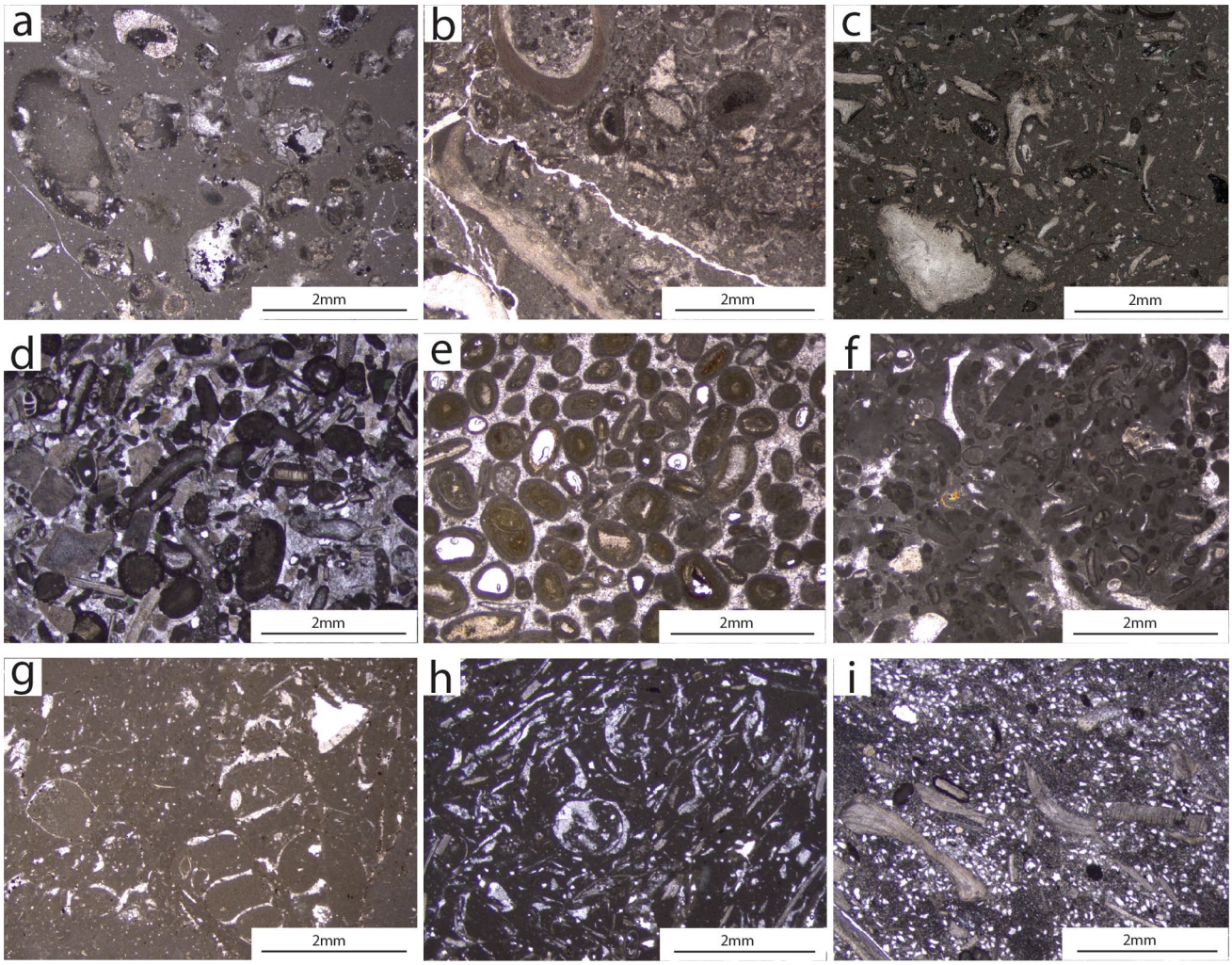


**Fig. 7** Microfacies types of Kimmeridgian successions in the study area. **a** MF type 2, wackestone with ramp-derived intraclasts, 16.2 m, Langenberg section. **b** MF type 3, bioclastic wacke to floatstone with oysters and serpulids, 13.9 m, Langenberg section. **c** MF type 4, bioclastic wackestone with abundant echinoderms and other bioclastic material, 9.8 m, Bisperode section. **d** MF type 5, bioclastic grainstone with abundant fossil fragments, 18.3 m, Bisperode section. **e** MF type 6, oolitic grainstone, 7.1 m, Langenberg section. **f** MF type 7, peloidal bioclastic wacke- to packstone with ostracods and foraminifera, 45.3 m, Langenberg section. **g** MF type 8, bioclastic floatstone with gastropods, 51.6 m, Langenberg section. **h** MF type 8, bioclastic wackestone with bivalves and gastropods 50.8 m, Bisperode section. **i** MF type 9, 17.3 m, sandy limestone with large mollusc fragments, Bisperode section

The association comprising MF types 7, 8 and 9 implies a transitional semi-restricted lagoon setting ranging from an open-marine to a restricted setting, which is characterized by moderate water energy and episodic terrestrial influx.

*MA5-a/b: Restricted lagoon depositional setting*

Depositional setting MA5-a/b is represented predominantly in the middle and upper parts of both sections. MF types of MA5-a include pelletal pack- to grainstone (MF type 10, Fig. 8a), bioclastic mud- to wackestone (MF type 11, Fig. 8b), peloidal sandy limestone (MF type 12, Fig. 8c) and limestone conglomerate (MF type 13, Fig. 8d), the latter being restricted to the uppermost part of the Langenberg section. MA5-b corresponds to shale–claystone alternations with sandy interbeds (MF type 14) restricted to a single interval in Bisperode (13.0–16.2 m).

A dominance of pellets and scarcity or absence of faunal elements indicate a hypersaline lagoonal setting with low-energy conditions and reduced sedimentation rates (Scholle and Ulmer-Scholle 2003; Flügel 2004). The occurrence of centimetre-scale woody debris (MF type 11) and sub-angular quartz (MF type 12) indicates a proximal setting. The intraclast-rich facies of MF type 13 (float- and rudstone in Baldermann et al. 2015) is composed of sub-rounded, centimetre- to decimetre-sized carbonate clasts.

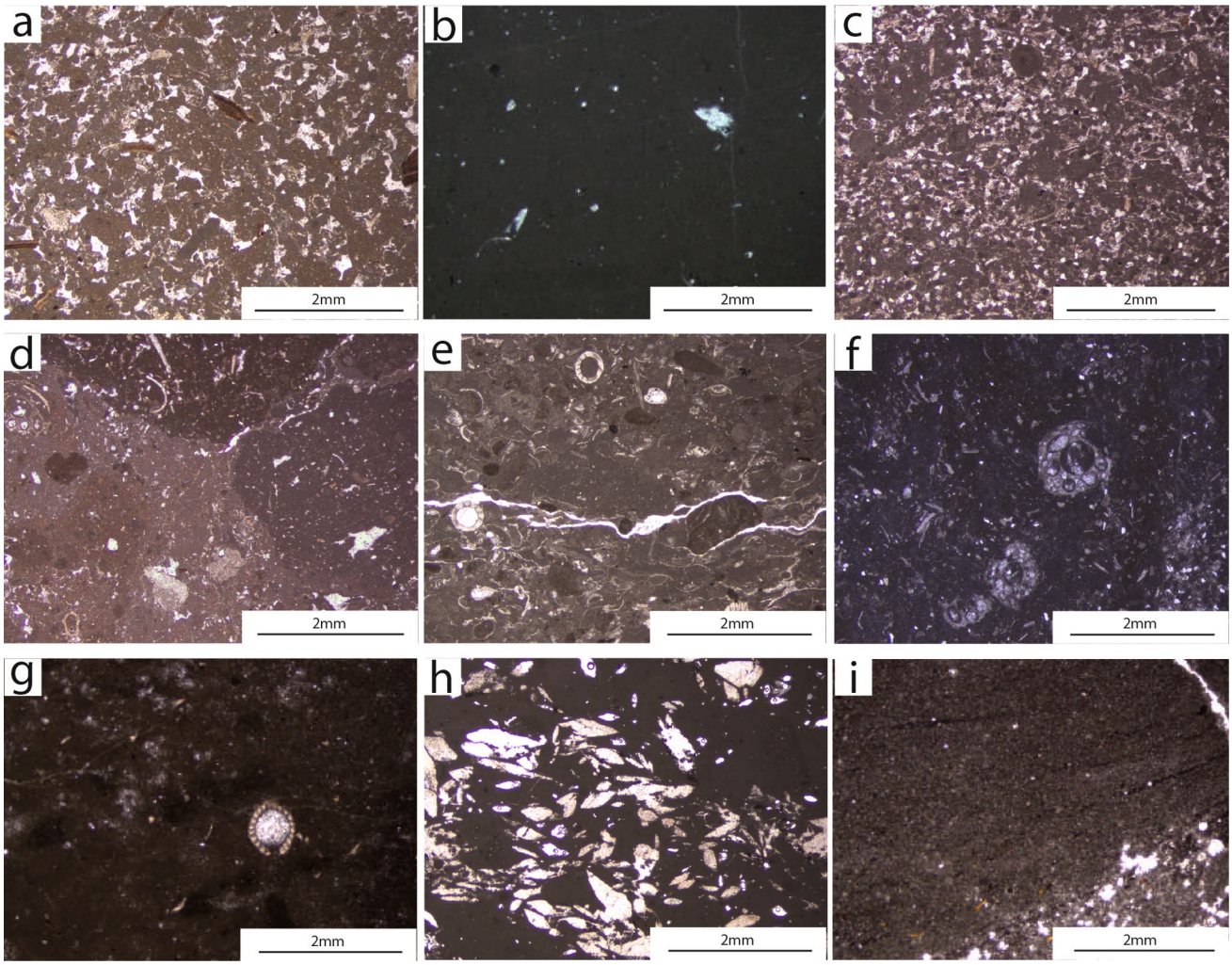


**Fig. 8** Microfacies types of Kimmeridgian successions in the study area. **a** MF type 10, pelletal grainstone, 72.7 m, Langenberg section. **b** MF type 11, mudstone, 1.4 m, Bisperode section. **c** MF type 12, peloidal sandy limestone, 33.7 m, Langenberg section. **d** MF type 13, limestone conglomerate, 73.8 m, Langenberg section. **e** MF type15, wackestone with charophytes and ostracods, 54.3 m, Langenberg section. **f** MF type 15, wackestone with charophytes, 41.8 m, Bisperode section. **g** MF type 16, charophyte-rich marlstone, 38.8 m, Langenberg section. **h** MF type 18, evaporite–dolomite couplets, 34.1 m, Langenberg section. **i** MF type 19, dolomitic mudstone, 67.5 m, Langenberg section

Both intraclasts and matrix contain rare bioclasts and compacted pellets and represent reworked debris flows. This is consistent with the interpretation of Fischer (1991), who suggested a storm-induced formation. In summary, MA5-a reflects deposition under low-energy, restricted subtidal lagoonal conditions, influenced by episodic storm events and reworking.

The shale–claystone alternations of MA5-b have a low carbonate content, a dark colour, thin bedding and intercalations of thin sandstone layers, which point to a subtidal lagoon setting receiving significant terrestrial influx during sea-level fall, climate change and/or tectonic activity (Bauer et al. 2002).

*MA6-a/b: Intertidal back-ramp depositional setting*

MA6-a/b occurs in the upper part of the Langenberg section and middle and upper parts of the Bisperode section and corresponds to mud- to wackestone with charophytes and ostracods (MA6-a: MF type 15, Fig. 8e, f), charophyte-rich marl or claystone (MA6-a: MF type 16, Fig. 8g) and fine-grained sandstone (MA6-b: MF type 17) (Table 1). Typically, MA6-a/b grades up into MA7 and overlies MA4 or MA5.

Ostracod carapaces can form substantial sedimentary constituents in restricted environments, especially in brackish, hypersaline, or freshwater settings (Scholle and

Ulmer-Scholle 2003). Charophyte remains are considered as indicators for fresh or brackish waters in coastal and non-marine environments (Scholle and Ulmer-Scholle 2003; Flügel 2004). Even though the combination of charophyte and ostracod remains within a micritic matrix in MA6-a may indicate a lacustrine environment (Cäsar 2012), its stratigraphic intercalation with lagoonal deposits suggests a brackish-water intertidal setting under low to medium hydrodynamic conditions (Flügel 2004). A peritidal setting is supported by the abundant occurrence of *Skolithos* in the upper part of the Langenberg section, probably formed by large crabs (Fischer 1991). Furthermore, finds of fish teeth of *Lissodus curvidens* n. sp. in the Langenberg section (bed 153) indicate reduced marine salinity and restricted conditions (Mudroch and Thies 1996; Duffin and Thies 1997; Mudroch et al. 1999; Thies et al. 2007).

Tidal-flat deposition under shallow-marine intertidal conditions is suggested by well-developed wave ripples in fine-grained sandstones (MA6-b), reflecting pulses of terrigenous siliciclastic influx derived from the hinterland during sea-level fall, climate change or tectonic activity (Walker and Plint 1992; Cäsar 2012).

*MA7: Supratidal back-ramp depositional setting*

MA7 is characterized by dolomitic deposits including evaporite–dolomite couplets (MF type 18, Fig. 8h) and dolomitic mudstone (MF type 19, Fig. 8i). MA7 is recorded in only three horizons in the middle and upper part of the Langenberg section.

According to Baldermann et al. (2015) and Rameil (2008), dolomitic limestone (mainly type A–C of Baldermann et al. 2015) is formed via early diagenetic replacement of micrite under slightly evaporative and reducing conditions in a carbonate tidal-flat setting during sea-level lowstand. A tidal-flat environment is also indicated by the remnants of microbial lamination and fenestral fabrics. Endocasts of the bivalve *Trigonia* sp. support a hypersaline scenario (Fischer 1991). Similarly, the occurrence of gypsum pseudomorphs (Fig. 8h) suggests formation in a supratidal sabkha under arid conditions (Flügel 2004; Colombié and Strasser 2005).

## Sedimentary model

Based on facies distribution and stratal architecture, the Upper Jurassic deposits in the LSB have been interpreted to be the product of a gently inclined carbonate ramp (Betzler et al. 2007; Kästner et al. 2008; Cäsar 2012). The sedimentary and carbonate microfacies inventory raised here enables the establishment of a detailed depositional model of the Kimmeridgian strata (Fig. 9). The spatial organization of different MAs along a proximal–distal transect reveals a hydrodynamic energy gradient (Kästner et al. 2008; Carcel et al. 2010; Sadeghi et al. 2011), which is a consequence of

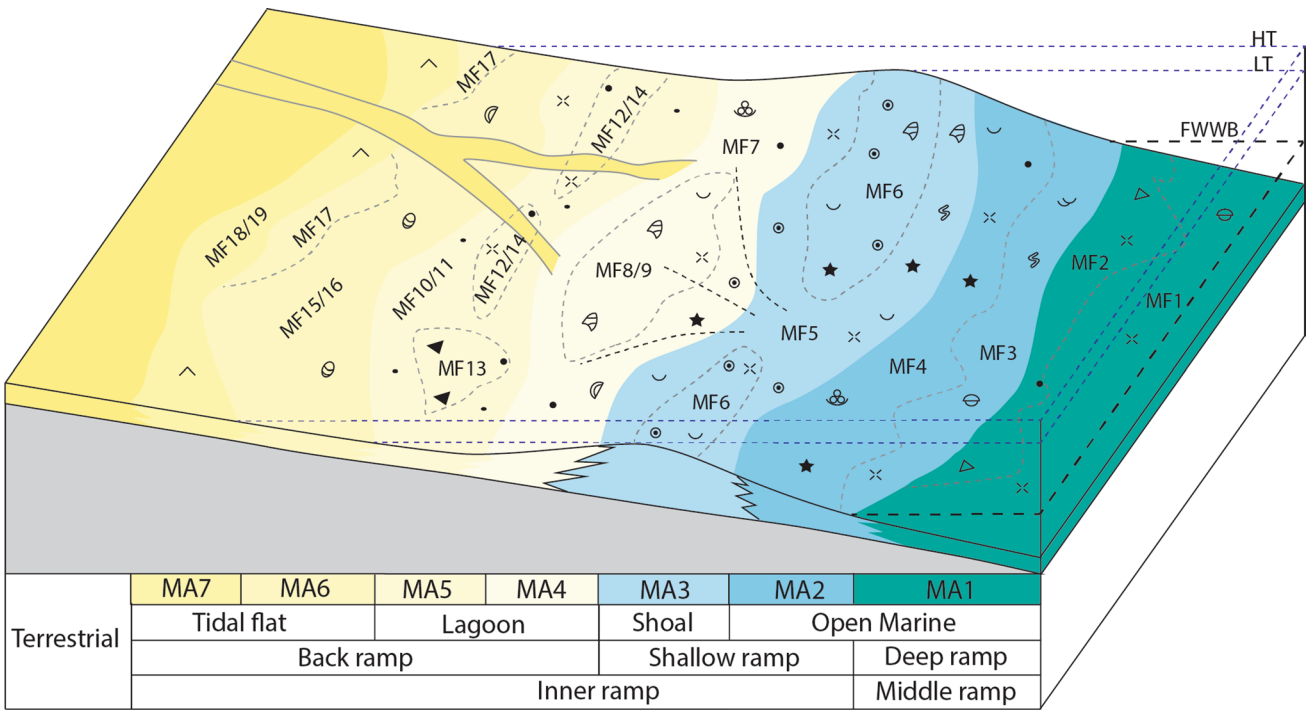


**Fig. 9** Model of the depositional setting for the Kimmeridgian successions in the study area (Lower Saxony Basin)

gradual depth changes and varying storm intensity (Tucker and Wright 1990; Wright and Burchette 1996; Flügel 2004).

Massive oolitic limestone and bioclastic pack- to grainstone of MA3 are interpreted as shoal deposits of the inner ramp formed under high-energy conditions (Flügel 2004; Betzler et al. 2007; Kästner et al. 2008). In a seaward direction, moderate- to low-energy conditions are indicated for the distal inner-ramp deposits formed close to the FWWB. In MA2, the composition of the biota indicates unrestricted, normal-marine conditions affected by storms, as shown by the tempestite beds composed of discrete shell accumulations (e.g. brachiopods, oysters). Deposits formed below the FWWB (MA1) are characterized by higher clay content, reduced species richness and intensified bioturbation, as well as redeposited inner-ramp-derived material. The occurrence of intraclasts containing ooids attests to reworking of shoal deposits and basinward transport into the mid-ramp facies belt (MA1) (Betzler et al. 2007). The deepest facies recorded in the mid-ramp is represented by marlstone containing an open-marine fauna and abundant *Thalassinoides* burrows.

In a landward direction, the back-ramp area is composed of a broad spectrum of depositional environments, including semi-restricted lagoon, restricted lagoon and tidal-flat settings. In the semi-restricted lagoon environment (MA4), a decrease in the variety of bioclasts is observed towards the lagoon centre. Monospecific mass accumulation of gastropods and bivalves points to high nutrient supply and/or changes in salinity (Reiss and Hottinger 1984). A more restricted and hostile lagoon environment is indicated by the scarcity or total absence of faunal remains and the dominance of pellets and fine-grained carbonate mud (MA5-a). Facies belts MA5 and MA4 have been moderately influenced by periodic siliciclastic input (MF9 and MF12). In the peritidal environment, an intertidal facies belt (MA6-a) containing abundant ostracod and charophyte remains indicates brackish conditions. The shale–claystone–sandstone alternations (MA5-b and MA6-b) indicate particular episodes of enhanced terrestrial shedding into the lagoonal and peritidal environment (e.g. McLaughlin et al. 2004; Kästner et al. 2008). In addition, a supratidal facies belt (MA7) characterized by dolomite and/or evaporite precipitation indicates subaerial exposure under a dry climate.

## Sequence stratigraphy

The sequence-stratigraphic interpretation of the Kimmeridgian succession in the LSB is based on the vertical stacking pattern of MF types, changes in bed thickness and the occurrence of diagnostic surfaces. This approach allows three orders of depositional sequence to be defined and provides a better understanding of the stratigraphic and spatial evolution of the sedimentary system. In view of the limited number of studied outcrops, the applied sequence-stratigraphic terminology follows Strasser et al. (1999), using lowstand, transgressive and highstand deposits instead of the systems tracts of Vail et al. (1991). In the following, only the Langenberg section is used as an example illustrating the small- and medium-scale sequences.

### *Small-scale sequences*

Small-scale depositional sequences as defined in the Langenberg section ($n = 30$) vary between 1.3 and 4.9 m in thickness, which is in accordance with the scheme proposed by Strasser et al. (1999). They show shallowing-up or deepening–shallowing trends of facies evolution and are bound by three types of diagnostic surface, including firm or hardgrounds (SB1), subaerial exposure surfaces (SB2) and surfaces capping the shallowest facies (SB3) (Fig. 10).

Complete shallowing–deepening small-scale sequences mainly occur in the lower part of the section, especially in the transgressive and maximum-flooding intervals of medium-scale sequences where accommodation space was high (Colombié and Strasser 2005). The deepening trend is normally characterized by a facies evolution towards more open conditions, with a change from distal inner-ramp (MA2/MA3) to mid-ramp settings (MA1), and a reverse interval indicating a shallowing trend. An exceptional slightly shallowing-up sequence (small-scale sequence 2, Fig. 10) composed of shoal deposits (MF type 6) is present in this interval, which is indicated by upward-thinning bed thickness and changes in carbonate content. Firm or hardgrounds representing SB1 mainly appear in this interval and are interpreted to confine so-called subtidal cycles (Ma et al. 1999; Strasser et al. 1999). SB1-type surfaces (e.g. top of sequences 2, 3 and 7) show colonization by encrusting oysters or intense bioturbation and/or borings (Fig. 3c and e), indicative of reduced sedimentation rates during sea-level fall or subsequent submergence. SB1 is typically overlain by thin-bedded marl formed as the result of increased clay supply due to erosion of the hinterland during sea-level fall or, alternatively, reflecting concentration of argillaceous material due to reduced carbonate production following a rapid sea-level rise (Strasser et al. 1999).

Asymmetric shallowing-up sequences, which are commonly observed in many ancient shallow-marine carbonate systems, mainly appear in the middle and upper part of the section and are interpreted as peritidal cycles (Ma et al. 1999; Strasser et al. 1999). Depositional environments mainly show gradual transitions from semi-restricted lagoon (MA4) to restricted lagoon (MA5) or tidal flat (MA6), or from open-marine settings (MA2/MA3) to lagoon and tidal flat. Typical boundaries in these peritidal cycles are represented by SB2- and SB3-type surfaces. Exposure and development of SB2-type boundaries (e.g. top of sequences 1, 13 and 25) are indicated by the dolomitization of the underlying

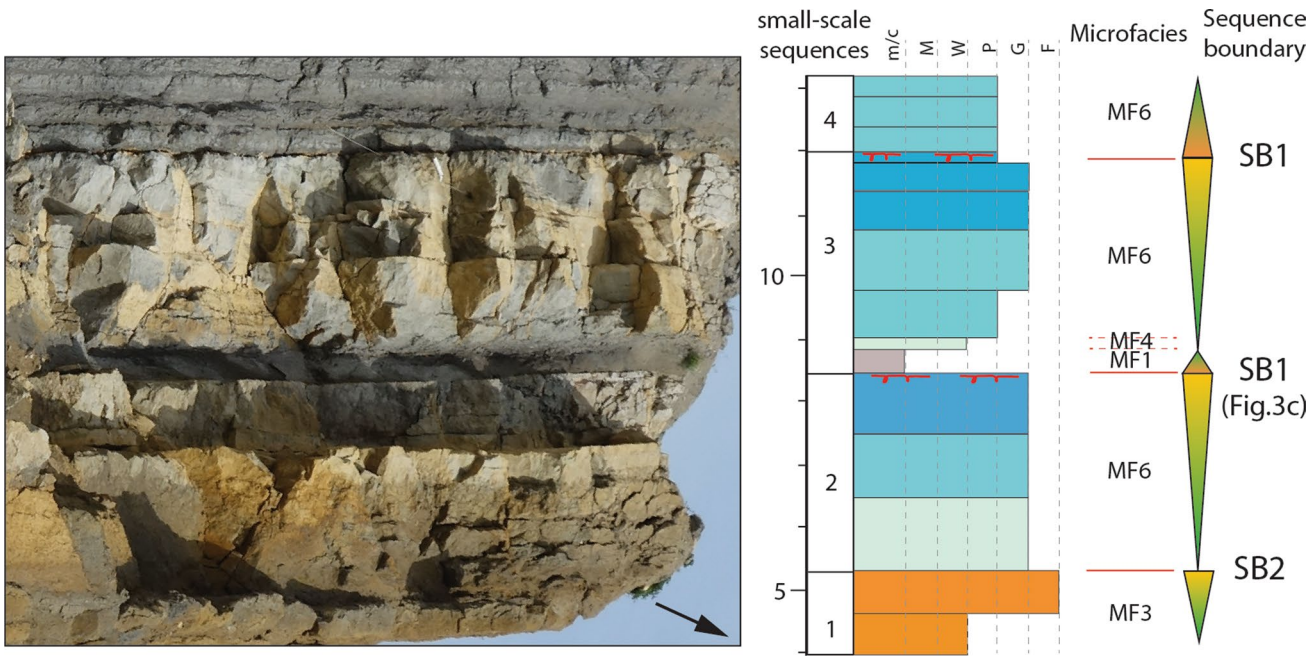


**Fig. 10** Outcrop photograph, textures and microfacies as well as sequence stratigraphy and boundaries developed in the lower part of the Langenberg section. The black arrow points to the vertical direction in the outcrop. Please refer to Fig. 4 for the symbols used here

strata, and usually developed during the late highstand of larger-scale sequences when accommodation was low (Colombié and Strasser 2005). SB3 is represented by sub- or intertidal surfaces that are capping the shallowest facies of the corresponding sequence. For instance, the boundary between sequences 19 and 20 is represented by the abrupt shift from the shallower MF type 11 to the deeper MF type 8 (Fig. 11). SB3 may represent both the sequence boundary and the transgressive surface, an observation that has been reported from many shallow-water carbonate platform settings where the respective lowstand deposits are not preserved (Strasser et al. 1999; Betzler et al. 2007).

*Medium-scale sequences*

In the Langenberg section, a total of seven medium-scale sequences can be recognized, each of which comprises two to six stacked small-scale sequences, resulting in a thickness range of 5.3 to 17.7 m (Fig. 11). Influenced by the Late Jurassic second-order transgression, the typical asymmetric sequential characteristic in shallow-marine carbonate systems is distorted or even reversed in the Kimmeridgian medium-scale sequences under study.

The lowermost medium-scale sequence 1 (0.0–5.3 m), composed of dolomitic and marly limestone, contains a thick maximum flooding deposit (MFD), which is characterized by MA1. The dolomite-rich interval indicates a period of exposure during relative sea-level fall (Sarg 2001; Rameil 2008; Baldermann et al. 2015). Medium-scale sequence 2 (5.3–12.0 m) comprises two small-scale sequences which are composed mainly of MF type 6 and capped by hardgrounds. Sequence 3 (12.0–20.1 m) is characterized by a well-developed transgressive part and a less-pronounced regressive interval. The lower deepening-upward subsequence is characterized by MF type 6, indicating shoal deposits, which are overlain by MF type 3 close to the FWWB. Relatively thick (~ 3 m) MFD show intense bioturbation and higher clay content. The overlying shallowing-upward subsequence shows a trend from a middle- to inner-ramp setting. The boundary between medium-scale sequences 3 and 4 is marked by a hardground and corresponds to a relative sea-level fall, resulting in a shift from open-marine towards more restricted facies, as indicated by MA4 to MA6. The maximum flooding interval of medium-scale sequence 4 (20.1–36.4 m) is composed of lagoonal and shoal facies (MA3 and MA4), whereas the overlying lagoon and tidal-flat deposits (MA4 to MA7) represent a well-developed regressive phase. The top is capped by a 2.5-m-thick dolomite interval, reflecting exposure during sea-level lowstand. A stratigraphic gap of ostracod zones 10 to 12 appears above this sequence, indicative of the major hiatus between the Lower Süntel and Middle Süntel Formations. Medium-scale sequence 5 (36.4–54.1 m) consists predominantly of lagoonal and intertidal facies (MA4 to MA6). A more distal setting is reflected by shoal sediments (MF type 5), which correspond to the MFD. Medium-scale sequence 6 (54.1–68.9 m) shows a well-developed

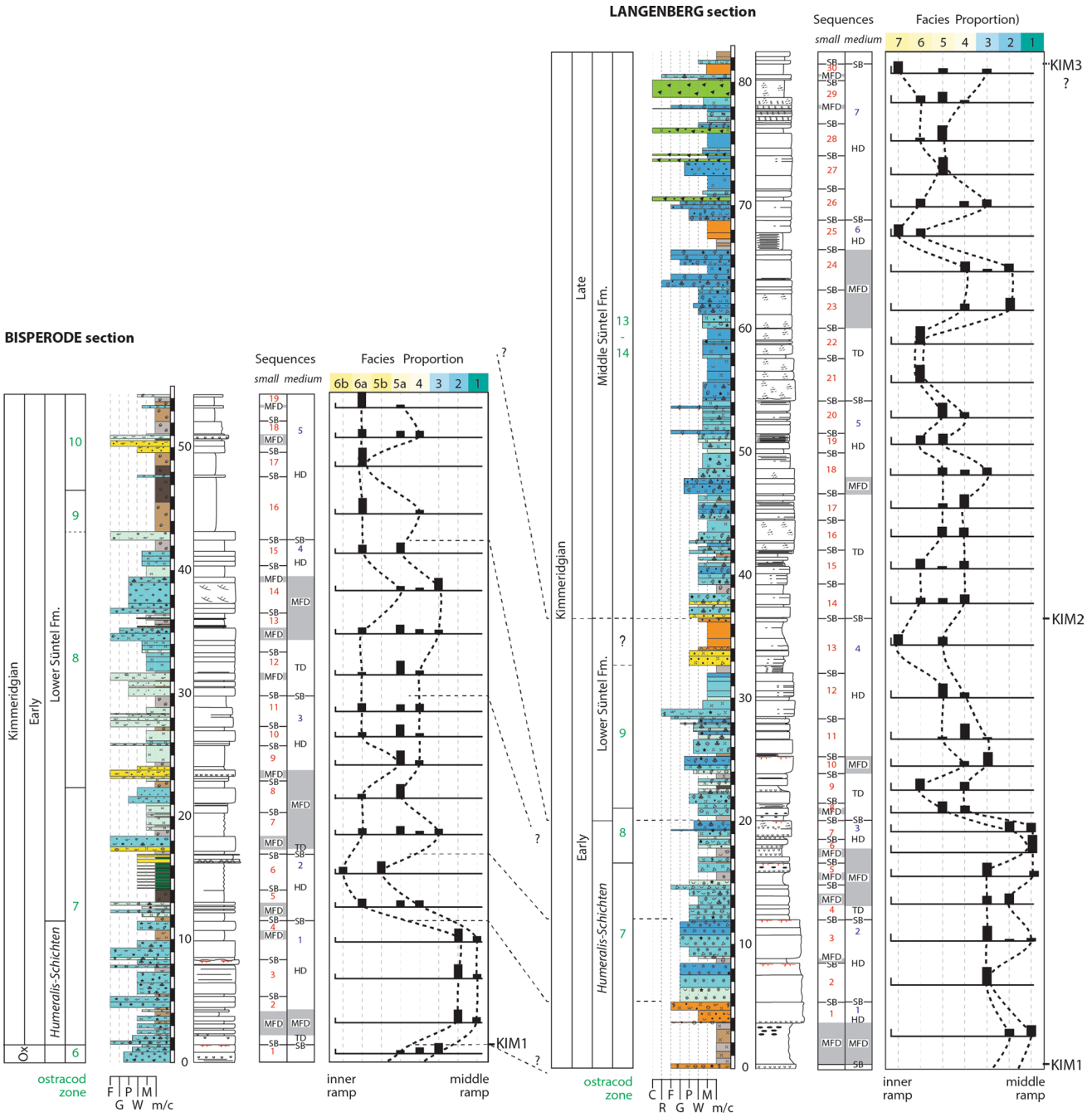


**Fig. 11** Correlation between Bisperode section and Langenberg section based on the sequence stratigraphy and microfacies as well as biostratigraphic constraints

deepening–shallowing trend, with its lower part reflecting a shift from tidal-flat to open-marine settings. MFD are represented by MF type 4, indicating a distal inner-ramp environment. This sequence is bound by replacement dolomite. Medium-scale sequence 7 (68.9–81.6 m) contains only a shallowing-upward interval consisting of shoal and back-shoal pack- to grainstone, with intercalated lagoonal facies containing several layers composed of MF type 13.

*Large-scale sequences*

Two large-scale sequences are defined by the stacking pattern of the medium-scale sequences in the Langenberg section. The lower one is bound by sequence boundaries KIM1 and KIM2 (Fig. 11). The deepening trend and the MFD correspond to medium-scale sequences 1–3, which are represented by MA1 to MA3, and the following shallowing trend

is characterized by a facies evolution from semi-restricted lagoon to tidal flat (MA4–MA7) in medium-scale sequence 4. A stratigraphic gap caused by erosion (as indicated by the lack of ostracod zones 10–12) results in the formation of sequence boundary KIM2 at 36.4 m. Above this surface, the deepening trend in the upper sequence shows a change from a restricted to open-marine setting, and the MFD is represented by MA2. The shallowing trend above is indicated by the reverse change back to more restricted environments. Constrained by ostracod biostratigraphy, the upper large-scale sequence in the Langenberg section can be correlated to the large-scale sequence 4 in Bai et al. (2017). The entire Bisperode section is part of a single large-scale sequence, which corresponds to the lower one in the Langenberg section. Only the lower sequence boundary KIM1 can be identified. Given the limited number of large-scale sequences covered by the studied succession, the stratigraphic correlation discussed in the following sections is dependent mainly on medium-scale sequences.

## Discussion

### Sedimentary evolution and correlation

Based on the integrated sedimentological and sequence-stratigraphic analysis outlined above, a preliminary correlation scheme for the Langenberg and Bisperode sections is proposed (Fig. 11). In particular, the integration of ostracod biostratigraphic results with sequence-stratigraphic interpretations illustrates the stratigraphic and spatial facies variations within the LSB.

In the Bisperode section, the Oxfordian–Kimmeridgian boundary (between ostracod zones 6 and 7) is represented by a discontinuity surface located at ~ 1.5 m. Medium-scale sequence 1 is characterized by mid-ramp and distal inner-ramp deposits in both the Bisperode and Langenberg sections. A shift towards inner-ramp oolitic shoal (Langenberg) or proximal lagoonal and tidal-flat environments (Bisperode) during medium-scale sequence 2 indicates a drop in relative sea level (Kendall and Schlager 1981; Jones and Desrochers 1992). Up-section, a gradual transgressive trend in both sections is documented by deposits ascribed to the upper part of ostracod zone 7 and ostracod zone 8 (medium-scale sequences 3 and 4 at Bisperode; medium-scale sequence 3 at Langenberg). During this interval, deposition evolves from inner to middle ramp at Langenberg, whereas it shifts from restricted back ramp to a shoal setting at Bisperode. In general, the Bisperode section reflects a more proximal position than the Langenberg section, which is also supported by the higher siliciclastic influence observed at Bisperode (Figs. 5 and 6). Notably, the overall sediment thickness and the number of sequences show significant differences between the two sections, especially in the stratigraphic interval ascribed to ostracod zone 8. According to Bádenas and Aurell (2001), the differences in both stratigraphic thickness and the number of sequences suggest that regional tectonic activity acts as an important factor in sequence development in the LSB. This interpretation is further supported by the sharp change from an open-marine towards a restricted depositional environment between sequences 3 and 4 in the Langenberg section, indicative of tectonic control on this episode of rapid accommodation loss (Bádenas and Aurell 2001). Above, the medium-scale sequence 5 in the Bisperode section is characterized by a thick charophyte-bearing mixed carbonate siliciclastic interval reflecting increasing terrestrial input into a restricted, near-coastal environment. Coeval sediments at Langenberg (Lower Süntel Formation, medium-scale sequence 4) form a thick deepening–shallowing cycle capped by dolomitic supratidal deposits, which mark the uppermost part of a shallowing-upward peritidal sequence (Rameil 2008; Baldermann et al. 2015). Furthermore, the stratigraphic gap between the Lower and Middle Süntel Formations (top of sequence 4), as indicated by the absence of ostracod zones 10 to 12, supports tectonic processes as an important controlling mechanism on the sediment distribution patterns. The Middle Süntel Formation as represented in the Langenberg section is composed of restricted back-ramp facies, with local intercalations of shoal deposits. Up-section, an increase in carbonate content reflects a decreasing continental influence, probably due to more arid conditions during the Late Kimmeridgian versus Early Kimmeridgian (Abbink et al. 2001; Carcel et al. 2010).

A tectonic influence on sequence development fits with the tectono-sedimentary evolution of the LSB. According to Gramann et al. (1997), the development of graben and half-graben structures started in the Oxfordian and intensified during the Kimmeridgian, resulting in the subdivision of the LSB into small troughs and swells, accompanied by thickness variations and lateral facies changes. A partly tectonic control on the spatial and stratigraphic facies distribution pattern of the Late Jurassic successions in the LSB has also been proposed by other authors (Betz et al. 1987; Gramann et al. 1997; Petmecky et al. 1999; Kley et al. 2008). A similar situation has been observed in the Iberian Basin, where Upper Kimmeridgian inner-ramp oolitic and reefal facies prograded over Early Kimmeridgian outer-ramp mudstone and marl triggered by local synsedimentary tectonics (Bádenas and Aurell 2001; Aurell et al. 2003). In summary, the observations reported in this study confirm the important role of regional synsedimentary tectonics in Kimmeridgian sedimentary development in the LSB.

## Sequence-stratigraphic implications

Gramann et al. (1997) revised and refined the biostratigraphic correlation scheme between the North German ostracod zonation and the Boreal standard ammonite zonation of Hardenbol et al. (1998). Thus, the biostratigraphic framework established here can be used to compare the sequence-stratigraphic scheme of the LSB with sequence-stratigraphic interpretations proposed for other Late Jurassic basins in Europe (Fig. 12). Top boundaries of sequences 3, 5, 6 and 7 and the basal boundaries of sequence 5 identified in the LSB appear coeval with sequence boundaries described from the Paris Basin (Lathuilière et al. 2015), the Wessex Basin (Taylor et al. 2001), the Jura Platform and the Vocontian Basin (Colombié and Strasser 2005), the Iberian Basin (Bádenas and Aurell 2001) and Southern Germany (Ruf et al. 2005).

Three medium-scale sequences can be recognized at the very onset (ostracod zones 7 and 8) of the Early Kimmeridgian in the LSB, but only a single sequence appears in comparable biostratigraphic positions in other European Basins (Fig. 12). Thus, top boundaries of sequences 1 and 2 in the LSB cannot be traced in other European Basins. According to Colombié and Strasser (2005) and Lathuilière et al. (2015), differences in the number of Kimmeridgian sequences among basins may result from the regional specificity of diagnostic sequence boundaries induced by differential synsedimentary tectonics and/or of deviating facies stacking patterns reflecting different sedimentary settings. In many European basins, the stratigraphic interval corresponding to the *Cymodoce* ammonite zone is marked by three to four medium-scale sequences. In contrast, the coeval interval in the LSB sections shows only a single sequence (sequence 4). The lack of more medium-scale sequences is best explained by erosion due to local tectonics in the LSB, which further underlines a regional tectonic control affecting the number of sequences. A major gap at this stratigraphic position is indicated by ostracod biostratigraphic results. The low biostratigraphic resolution of this particular interval (imprecisely assigned to ostracod zones 9 to 12) hampers the comparison and correlation of the top boundaries of sequence 4. Furthermore, the ambiguity in the correlation between Tethyan and Boreal ammonite zonation schemes may also explain the above-mentioned

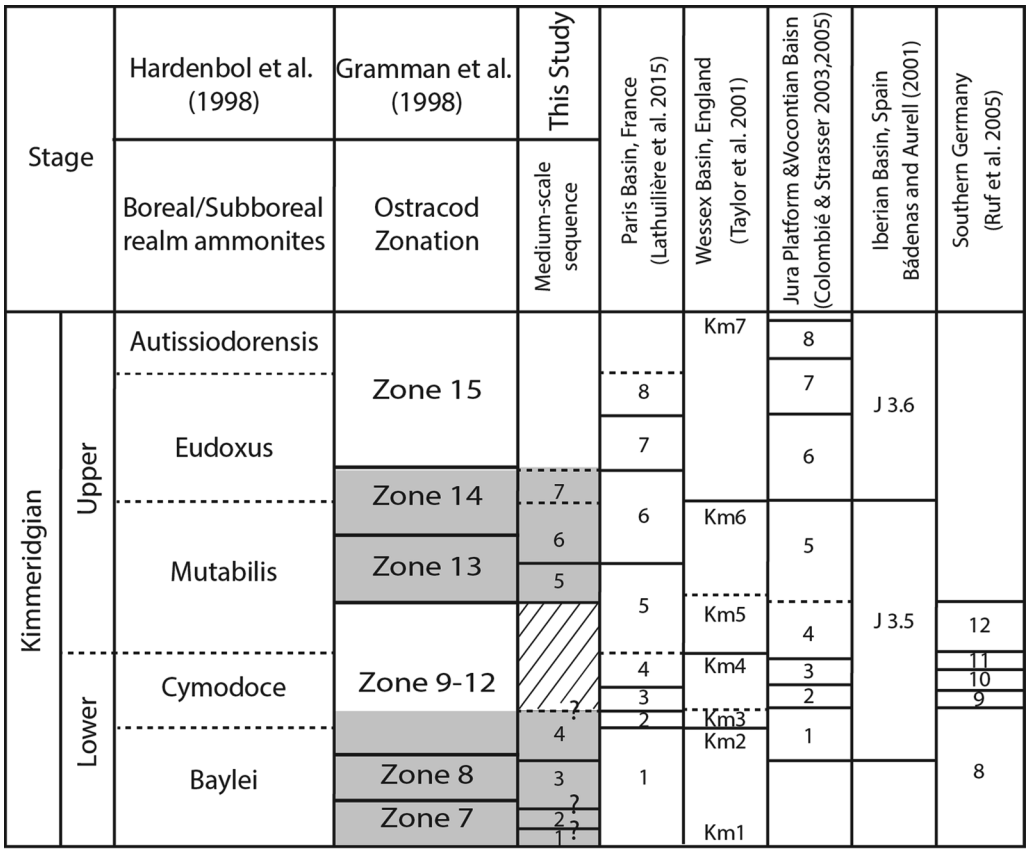


**Fig. 12** Comparison between the sequence-stratigraphic interpretation proposed in this study with those defined in other Late Jurassic basins in Europe (modified from Colombié and Strasser 2005; Ruf et al. 2005; Lathuilière et al. 2015). The uncertainty positions of some boundaries are noted as dashed lines and the greyish intervals represent the strata covered in this study

deviations or discrepancies to some extent (Colombié and Strasser 2005).

The Late Jurassic was characterized by a second-order transgression, which began in the Late Oxfordian and reached its maximum in the Late Kimmeridgian (Hardenbol et al. 1998; Hallam 2001; Miller et al. 2005; Ogg et al. 2012). In many western European basins, this major sea-level rise led to the formation of marly and/or condensed sections (e.g. Wessex Basin, England: Morgans-Bell et al. 2001; Taylor et al. 2001; Williams et al. 2001; Paris Basin, France: Lathuilière et al. 2015) and deeper-water carbonates (southern Germany, Ruf et al. 2005), all of which reveal a consistent deepening trend during the Kimmeridgian. However, the latter trend contrasts with the relative sea-level evolution in the LSB established herein. The observed overall shallowing trend from mid-ramp towards back-ramp settings implies that sediment production and supply in the LSB were faster than the formation of accommodation space during the second-order sea-level rise (Kendall and Schlager 1981; Jones and Desrochers 1992; Posamentier et al. 1992; Hunt and Tucker 1995; Carcel et al. 2010), resulting in progradation of the ramp during the Kimmeridgian. A similar scenario of ongoing carbonate platform progradation during the Early and early Late Kimmeridgian due to continuously high carbonate production was observed on the Swiss Jura platform as well as in the Vocontian Basin (Colombié and Strasser 2003, 2005). Therefore, high carbonate production (Figs. 5 and 6) must be an important factor controlling the shallowing trend of the Kimmeridgian strata in the LSB.

## Conclusions

1. Detailed lithological logs are presented for two Upper Jurassic sections (Langenberg, Bisperode) located in the LSB in northern Germany. Although open-marine marker fossils (i.e. ammonites) are scarce in Kimmeridgian strata of the LSB, ostracod biostratigraphy enabled precise age assignment and correlation of the sections studied. Whereas the Langenberg section comprises strata ranging from the *Humeralis-Schichten* (Uppermost Korallenoolith, ostracod zones 7–8) to the Middle Süntel Formation (ostracod zones 13–14), the Bisperode section comprises only the *Humeralis-Schichten* (lower part of ostracod zone 7) and only part of the Lower Süntel Formation (ostracod zones 7–10).
2. Based on field observations and thin-section analysis, 19 microfacies (MF) types are defined and attributed to seven microfacies associations (MAs), which are assigned to a carbonate ramp model ranging from mid-ramp to restricted proximal inner-ramp settings. Facies reveal that lagoonal and peritidal deposits (MA4-7) and intercalated high-energy shoal sediments (MA3) dominate most of the Kimmeridgian successions under study. More open-marine facies representing distal inner-ramp (MA2) and mid-ramp deposits (MA1) appear only in the lower part of both sections.
3. Stacking pattern of small-, medium- and large-scale sequences are defined based on the vertical microfacies stacking pattern, bed thickness and diagnostic sequence boundaries. Small-scale sequences in the Langenberg ($n = 30$) and Bisperode ($n = 19$) sections (thickness: 1.3–4.9 m) show shallowing-up and deepening-shallowing trends capped by three kinds of surface. Seven (Langenberg) and five (Bisperode) medium-scale sequences (thickness: 5.3–17.7 m) are identified and can be used for correlation based on the biostratigraphic framework. Two and one large-scale sequence are recognized in Langenberg and Bisperode sections, respectively.
4. The detailed sedimentary and sequence-stratigraphic analysis reveals that Bisperode reflects a more proximal setting than Langenberg. Regressive or transgressive trends within the medium-scale sequences correlate well between the two sections, both of which show an overall shallowing trend with stratigraphic height.
5. Regional synsedimentary tectonics is regarded as an important controlling factor for the differential sedimentation patterns of the Kimmeridgian deposits in the LSB. In addition, high carbonate production is suggested to have been responsible for keeping up with the creation of accommodation space and resulted in the progradation of Kimmeridgian successions (Süntel Formation) in the LSB.
6. Most of the medium-scale sequence boundaries defined in this study occur in similar biostratigraphic positions in other European basins. Observed deviations between different basins are probably caused by regionally differing tectonic activity, the inaccuracies of the applied biostratigraphic schemes and the ambiguity related to the correlation between the Tethyan and Boreal realms.

**Acknowledgments** We would like to thank Rohstoffbetriebe Oker GmbH & Co. KG and Hannoversche Basaltwerke GmbH & Co. KG for access to quarries and support during the field and sampling campaign. For insightful discussions, we thank H.Q. Bai and C. Betzler (Univ. Hamburg). We also thank Claude Colombié and Beatriz Bádenas for constructive and helpful reviews that improved an earlier draft of the manuscript. The China Scholarship Council (CSC) is gratefully acknowledged for financial support provided to F. Zuo.

## References

Abbink O, Targarona J, Brinkhuis H, Visscher H (2001) Late Jurassic to earliest Cretaceous palaeoclimatic evolution of the southern North Sea. Glob Planet Change 30:231–256

Alberti M, Fürsich FT, Abdelhady AA, Andersen N (2017) Middle to Late Jurassic equatorial seawater temperatures and latitudinal temperature gradients based on stable isotopes of brachiopods and oysters from Gebel Maghara. Egypt. Palaeogeogr Palaeoclimatol Palaeoecol 468:301–313

André J, Biagi R, Moguedet G, Buffard R, Clément G, Redois F, Baloge PA (2003) Mixed siliciclastic cool-water carbonate deposits over a tide-dominated epeiric platform: the Faluns of l'Anjou formation (Miocene, W. France). Annales de paléontologie 89:113–123

Aurell M, Robles S, Bádenas B, Rosales I, Quesada S, Meléndez G, García-Ramos J (2003) Transgressive–regressive cycles and Jurassic palaeogeography of northeast Iberia. Sediment Geol 162:239–271

Bádenas B, Aurell M (2001) Kimmeridgian palaeogeography and basin evolution of northeastern Iberia. Palaeogeogr Palaeoclimatol Palaeoecol 168:291–310

Bai HQ, Betzler C, Erbacher J, Reolid J, Zuo F (2017) Sequence stratigraphy of Upper Jurassic deposits in the North German Basin (Lower Saxony, Süntel Mountains). Facies 63(3):19

Baldermann A, Grathoff GH, Nickel C (2012) Micromilieu-controlled glauconitization in fecal pellets at Oker (Central Germany). Clay Miner 47:513–538

Baldermann A, Deditius AP, Dietzel M, Fichtner V, Fischer C, Hippler D, Leis A, Baldermann C, Mavromatis V, Stickler CP, Strauss H (2015) The role of bacterial sulfate reduction during dolomite precipitation: implications from Upper Jurassic platform carbonates. Chem Geol 412:1–14

Bauer J, Kuss J, Steuber T (2002) Platform environments, microfacies and systems tracts of the Upper Cenomanian-lower Santonian of Sinai. Egypt. Facies 47:1–25

Betz D, Führer F, Greiner G, Plein E (1987) Evolution of the Lower Saxony Basin. Tectonophysics 137:127–170

Betzler C, Pawellek T, Abdullah M, Kossler A (2007) Facies and stratigraphic architecture of the Korallenoolith Formation in North Germany (Lauensteiner Pass, Ith Mountains). Sediment Geol 194:61–75

Burchette TP, Wright VP, Faulkner TJ (1990) Oolitic sandbody depositional models and geometries, Mississippian of southwest Britain: implications for petroleum exploration in carbonate ramp settings. Sediment Geol 68:87–115

Carballido JL, Sander PM (2013) Postcranial axial skeleton of *Europasaurus holgeri* (Dinosauria, Sauropoda) from the Upper Jurassic of Germany: implications for sauropod ontogeny and phylogenetic relationships of basal Macronaria. J Syst Paleontol 12:335–387

Carcel D, Colombié C, Giraud F, Courtinat B (2010) Tectonic and eustatic control on a mixed siliciclastic–carbonate platform during the Late Oxfordian-Kimmeridgian (La Rochelle platform, western France). Sediment Geol 223:334–359

Cäsar S (2012) Sequenzstratigraphie und sedimentologie oberjurassischer Karbonate von Norddeutschland (Oxfordium/Kimmeridgium, Niedersächsisches Becken). Dissertation, Universität Hamburg

Colombié C, Rameil N (2007) Tethyan-to-boreal correlation in the Kimmeridgian using high-resolution sequence stratigraphy (Vocontian Basin, Swiss Jura, Boulonnais, Dorset). Int J Earth Sci (Geol Rundsch) 96:567–591

Colombié C, Strasser A (2003) Depositional sequences in the Kimmeridgian of the Vocontian Basin (France) controlled by carbonate export from shallow-water platforms. Geobios 36:675–683

Colombié C, Strasser A (2005) Facies, cycles, and controls on the evolution of a keep-up carbonate platform (Kimmeridgian, Swiss Jura). Sedimentology 52:1207–1227

Dauwalder P, Remane J (1979) Etude du Banc à nérinées à la limite « kimmeridgien-portlandien » dans le jura Neuchâtelois méridional. Paläontol Z 53:163–181

Diedrich C (2009) Stratigraphy, fauna, palaeoenvironment and palaeocology of the Stollenbank Member (Süntel Formation, mutabilis/eudoxus zonal boundary, KIM 4, Upper Kimmeridgian) of NW Germany. Neues Jahrbuch für Geologie und Paläontologie-Abhandlungen 252:327–359

Duffin CJ, Thies D (1997) Hybodont shark teeth from Kimmeridgian (Late Jurassic) of northwest Germany. Geol Palaeontol 31:235–256

Dunham RJ (1962) Classification of carbonate rocks according to depositional texture. In: Ham WE (ed) Classification of carbonate rocks, vol 1. AAPG, Tulsa, pp 108–121

Dupraz C, Strasser A (1999) Microbialites and micro-encrusters in shallow coral bioherms (Middle to Late Oxfordian, Swiss Jura mountains). Facies 40:101–129

Embry AF III, Klovan JE (1971) A Late Devonian reef tract on northeastern Banks Island, NWT. Bull Can Pet Geol 19:730–781

Fischer R (1991) Die Oberjura: Schichtfolge vom Langenberg bei Oker. Arbeitskreis Paläontologie Hannover 19:21–36

Flügel E (2004) Microfacies of carbonate rocks, 2nd edn. Springer, Heidelberg

Gerke O, Wings O (2016) Multivariate and cladistic analyses of isolated teeth reveal sympatry of theropod dinosaurs in the Late Jurassic of Northern Germany. PLoS One 11:e0158334

Gradstein FM, Ogg JG (2012) The chronostratigraphic scale. In: Gradstein FM, Ogg JG, Schmitz MD, Ogg GM (eds) The Geologic time scale 2012, vol 2. Elsevier, p 32

Gramann F, Luppold FW (1991) Zur Mikropaläontologie des oberen Jura im Autobahn-Einschnitt Uppen, östlich Hildesheim, und der Grenze Korallenoolith-Kimmeridge in Niedersachsen. Geologisches Jahrbuch A 126:197–233

Gramann F, Heunisch C, Klassen H, Kockel F, Dulce G, Harms F, Katschorek T, Mönnig E, Schudack M, Schudack U, Thies D, Weiss M (1997) Das Niedersächsische Oberjura-Becken-Ergebnisse Interdisziplinärer Zusammenarbeit. Zeitschrift der Deutschen Geologischen Gesellschaft 148:165–236

Hallam A (1993) Jurassic climates as inferred from the sedimentary and fossil record. Philos Trans R Soc Lond 341:287–293

Hallam A (2001) A review of the broad pattern of Jurassic sea-level changes and their possible causes in the light of current knowledge. Palaeogeogr Palaeoclimatol Palaeoecol 167:23–37

Hardenbol J, Thierry J, Farley MB, Jacquin T, de Graciansky PC and Vail PR (1998) Jurassic chronostratigraphy. In: de Graciansky PC, Hardenbol J, Jacquin T, Vail PR (eds) Mesozoic and cenozoic sequence stratigraphy of European Basins. SEPM Special Publication, Tulsa, pp 3–13

Helm C (2005) Riffe und fazielle Entwicklung der florigemma-Bank (Korallenoolith, Oxfordium) im Süntel und östlichen Wesergebirge (NW-Deutschland). Geol Beitr Hann 7:10–339

Helm C, Schülke I (1998) A coral-microbialite patch reef from the Late Jurassic (florigemma-Bank, Oxfordian) of NW Germany (Süntel mountains). Facies 39:75–104

Helm C, Schülke I (2006) Patch reef development in the florigemma-Bank Member (Oxfordian) from the Deister Mts (NW Germany): a type example for Late Jurassic coral thrombolite thickets. Facies 52:441–467

Helm C, Reuter M, Schülke I (2003) Die Korallenfauna des Korallenooliths (Oxfordium, Oberjura, NW-Deutschland): zusammensetzung, Stratigraphie und regionale Verbreitung. Paläontol Z 77:77–94

Hesselbo SP, Deconinck J, Huggett JM, Morgans-Bell HS (2009) Late Jurassic palaeoclimatic change from clay mineralogy and gamma-ray spectrometry of the Kimmeridge Clay, Dorset, UK. J Geol Soc 166:1123–1133

Hine AC (1977) Lily Bank, Bahamas: history of an active oolite sand shoal. J Sediment Res 47:1554–1582

Hoyer P (1965) Fazies, Paläogeographie und Tektonik des Malm im Deister,-Osterwald und Süntel. Beih Geol Jb 61:249

Hunt D, Tucker ME (1995) Stranded parasequences and the forced regressive wedge systems tract: deposition during base-level fall—reply. Sediment Geol 95:147–160

Jansen M, Klein N (2014) A juvenile turtle (Testudines, Eucryptodira) from the Upper Jurassic of Langenberg Quarry, Oker, Northern Germany. Palaeontology 57:743–756

Jones B, Desrochers A (1992) Shallow platform carbonates. In: Walker RG, James NP (eds) Facies Models. Response to Sea Level Change, Geol Assoc Canada, pp 277–301

Karl HV, Gröning E, Brauckmann C, Schwarz D, Knötschke N (2006) The Late Jurassic crocodiles of the Langenberg near Oker, Lower Saxony (Germany), and description of related materials (with remarks on the history of quarrying the "Langenberg Limestone" and "Obernkirchen Sandstone"). Clausthaler Geowiss 5:59–77

Kästner M, Schülke I, Winsemann J (2008) Facies architecture of a Late Jurassic carbonate ramp: the Korallenoolith of the Lower Saxony Basin. Int J Earth Sci (Geol Rundsch) 97:991–1011

Kästner M, Schülke I, Winsemann J, Böttcher J (2010) High-resolution sequence stratigraphy of a Late Jurassic mixed carbonate-siliciclastic ramp, Lower Saxony Basin, Northwestern Germany. Z dt Ges Geowiss 16:263–283

Kendall CGStC, Schlager W (1981) Carbonates and relative changes in sea level. Mar Geol 44:181–212

Kerans C, Tinker SW (1997) Sequence stratigraphy and characterization of carbonate reservoirs. SEPM Short Course 40:1–130

Kley J, Franzke HJ, Jähne F et al (2008) Strain and stress. In: Bayer U, Gajewski D, Nelskamp S (eds) Littke R. Dynamics of complex intracontinental basins: The Central European Basin System, Springer, pp 97–124

Krajewski M, Olchowy P, Felisiak I (2016) Late Jurassic facies architecture of the Złoczew Graben: implications for evolution of the tectonic-controlled northern peri-Tethyan shelf (Upper Oxfordian-Lower Kimmeridgian, Poland). Facies 62:4

Lallensack JN, Sander PM, Knötschke N, Wings O (2015) Dinosaur tracks from the Langenberg Quarry (Late Jurassic, Germany) reconstructed with historical photogrammetry: evidence for large theropods soon after insular dwarfism. Palaeontol Electron 18:1–34

Lathuilière B, Bartier D, Bonnemaison M et al (2015) Deciphering the history of climate and sea level in the Kimmeridgian deposits of Bure (eastern Paris Basin). Palaeogeogr Palaeoclimatol Palaeoecol 433:20–48

Lécuyer C (2003) Thermal evolution of Tethyan surface waters during the Middle-Late Jurassic. Paleoceanography 18:1

Luppold FW (2003) Neue und seltene Index-Foraminiferen und -Ostrakoden aus dem Jura NW-Deutschlands. Senckenb Lethaea 83:15–37

Ma YS, Mei MX, Chen XB, Wang GW, Zhou L (1999) Sedimentology of carbonate reservoirs. Geological Publishing House, Beijing

Malchus N, Steuber T (2002) Stable isotope records (O, C) of Jurassic aragonitic shells from England and NW Poland: palaeoecological and environmental implications. Geobios 35:29–39

Marpmann JS, Carballido JL, Sander PM, Knötschke N (2014) Cranial anatomy of the Late Jurassic dwarf sauropod *Europasaurus holgeri* (Dinosauria, Camarasauromorpha): ontogenetic changes and size dimorphism. J Syst Paleont 13:221–263

Martin JE, Amiot R, Lécuyer C, Benton MJ (2014) Sea surface temperature contributes to marine crocodylomorph evolution. Nat Commun 5:4658

Martin T, Schultz JA, Schwermann AH, Wings O (2016) First Jurassic mammals of Germany: multituberculate teeth from the Late Jurassic Langenberg Quarry near Goslar (Lower Saxony). Acta Palaeontol Pol 67:171–179

McLaughlin PI, Brett CE, Taha McLaughlin SL, Cornell SR (2004) High-resolution sequence stratigraphy of a mixed carbonate-siliciclastic, cratonic ramp (Upper Ordovician; Kentucky-Ohio, USA): insights into the relative influence of eustasy and tectonics through analysis of facies gradients. Palaeogeogr Palaeoclimatol Palaeoecol 210:267–294

Miller KG, Kominz MA, Browning JV, Wright JD, Mountain GS, Katz ME, Sugarman PJ, Cramer BS, Christie-Blick N, Pekar SF (2005) The Phanerozoic record of global sea-level change. Science (New York, N.Y.) 310:1293–1298

Morgans-Bell HS, Coe AL, Hesselbo SP, Jenkyns HC, Weedon GP, Marshall JEA, Tyson RV, Williams CJ (2001) Integrated stratigraphy of the Kimmeridge Clay Formation (Upper Jurassic) based on exposures and boreholes in south Dorset, UK. Geol Mag 138:511–539

Mudroch A, Thies D (1996) Knochenfichzähne (Osteichthyes, Actinopterygii) aus dem Oberjura (Kimmeridgian) des Langenbergs bei Oker (Norddeutschland). Geol Palaeontol 30:239–265

Mudroch A, Thies D, Baumann A (1999) $^{87}Sr/^{86}Sr$ analysis on Late Jurassic fish teeth. Implication for paleosalinity of fossil habitats. In: Arratia G (ed) Mesozoic Fishes—Systematics and Fossil Record. Proceedings of the 2nd International Meeting, Buckow 1997, pp 595–604

Nunn EV, Price GD (2010) Late Jurassic (Kimmeridgian–Tithonian) stable isotopes ($\delta^{18}O$, $\delta^{13}C$) and Mg/Ca ratios: new palaeoclimate data from Helmsdale, northeast Scotland. Palaeogeogr Palaeoclimatol Palaeoecol 292:325–335

Ogg JG, Hinnov LA, Huang C (2012) Jurassic. In: Gradstein FM, Ogg JG, Schmitz MD, Ogg GM (eds) The geologic time scale 2012, vol 2. Elsevier, Amsterdam, pp 731–791

Pearce CR, Coe AL, Cohen AS (2010) Seawater redox variations during the deposition of the Kimmeridge Clay Formation, United Kingdom (Upper Jurassic): evidence from molybdenum isotopes and trace metal ratios. Paleoceanography 25:PA4213

Petmecky S, Meier L, Reiser H, Littke R (1999) High thermal maturity in the Lower Saxony Basin: intrusion or deep burial? Tectonophysics 304:317–344

Pettijohn FJ, Potter PE, Siever R (1987) Sand and sandstones. Springer, New York

Pieńkowski G, Schudack ME, Bosák P et al (2008) Jurassic. In: McCann T (ed) The geology of central Europe. Mesozoic and cenozoic, 2nd edn. Geological Society, London, p 869

Posamentier HW, Allen GP, James DP, Tesson M (1992) Forced regressions in a sequence stratigraphic framework: concepts, examples, and exploration significance (1). AAPG Bull 76:1687–1709

Rameil N (2008) Early diagenetic dolomitization and dedolomitization of Late Jurassic and earliest Cretaceous platform carbonates. A case study from the Jura Mountains (NW Switzerland, E France). Sediment Geol 212:70–85

Reiss Z, Hottinger L (1984) The Gulf of Aqaba: ecological micropaleontology. Springer, Berlin

Reolid M, Gaillard C, Olóriz F, Rodríguez-Tovar FJ (2005) Microbial encrustations from the Middle Oxfordian-earliest Kimmeridgian lithofacies in the Prebetic Zone (Betic Cordillera, southern Spain): characterization, distribution and controlling factors. Facies 50:529–543

Riboulleau A, Baudin F, Daux V, Hantzpergue P, Renard M, Zakharov V (1998) Evolution de la paléotempérature des eaux de la plateforme russe au cours du Jurassique supérieur. Comptes Rendus de l'Académie des Sci Ser IIA-Earth Planet Sci 326:239–246

Ruf M, Link E, Pross J, Aigner T (2005) Integrated sequence stratigraphy: facies, stable isotope and palynofacies analysis in a deeper

epicontinental carbonate ramp (Late Jurassic, SW Germany). Sediment Geol 175:391–414
Sadeghi R, Vaziri-Moghaddam H, Taheri A (2011) Microfacies and sedimentary environment of the Oligocene sequence (Asmari Formation) in Fars sub-basin, Zagros Mountains, southwest Iran. Facies 57:431–446
Sander PM, Mateus O, Laven T, Knötschke N (2006) Bone histology indicates insular dwarfism in a new Late Jurassic sauropod dinosaur. Nature 441:739–741
Sarg JF (2001) The sequence stratigraphy, sedimentology, and economic importance of evaporite-carbonate transitions: a review. Sediment Geol 140:9–34
Schmid DU (1996) Marine Mikrobolithe und Mikroinkrustierer aus dem Oberjura. Profil 9:101–251
Scholle PA, Ulmer-Scholle DS (2003) A color guide to the petrography of carbonate rocks: grains, textures, porosity. Diagenesis, AAPG
Schudack ME (1993) Die charophyten in oberjura und unterkreide westeuropas: mit einer phylogenetischen analyse der gesamtgruppe. Berl Geowiss Abh E8:1–209
Schudack U (1994) Revision, Dokumentation und Stratigraphie der Ostracoden des nordwestdeutschen Oberjura und Unter-Berriasium. Berl Geowiss Abh E11:1–193
Schudack ME (1996) Die Charophyten des Niedersächsischen Beckens (Oberjura-Berriasium): lokalzonierung, überregionale Korrelation und Palökologie. Neues Jb Geol Paläontol Abh 200:27–52
Schweigert G (1996) Historische Ammonitenfunde an der Porta Westfalica und deren Bedeutung für die Stratigraphie des nordwestdeutschen Oberjura. Osnabrücker Naturwissenschaftliche Mitteilungen 22:23–34
Schweigert G (1999) Neue biostratigraphische Grundlagen zur Datierung des nordwestdeutschen höheren Malm. Osnabrücker Naturwissenschaftliche Mitteilungen 25:25–40
Sellwood BW, Valdes PJ (2008) Jurassic climates. Proc Geol Assoc 119:5–17
Senglaub Y, Littke R, Brix MR (2006) Numerical modelling of burial and temperature history as an approach for an alternative interpretation of the Bramsche anomaly, Lower Saxony Basin. Int J Earth Sci (Geol Rundsch) 95:204–224
Strasser A, Pittet B, Hillgärtner H, Pasquier J (1999) Depositional sequences in shallow carbonate-dominated sedimentary systems: concepts for a high-resolution analysis. Sediment Geol 128:201–221
Taylor SP, Sellwood BW, Gallois RW, Chambers MH (2001) A sequence stratigraphy of the Kimmeridgian and Bolonian stages (late Jurassic): wessex-Weald Basin, southern England. J Geol Soc 158:179–192
Thies D, Mudroch A, Turner S (2007) The potential of vertebrate microfossils for marine to non-marine correlation in the Late Jurassic. Prog Nat Sci 17:79–87
Tucker ME, Wright VP (1990) Carbonate Sedimentology. Blackwell, Oxford
Vail PR, Audemard F, Bowman SA, Eisner PN, Perez-Crus C (1991) The stratigraphic signatures of tectonics, eustasy and sedimentology-an overview. In: Einseke G, Ricken W, Seilacher A (eds) Cycles Events Stratigraphy. Springer-Verlag, Berlin, pp 617–659
Valdes PJ, Sellwood BW (1992) A palaeoclimate model for the Kimmeridgian. Palaeogeogr Palaeoclimatol Palaeoecol 95:47–72
van Hinsbergen DJJ, de Groot LV, van Schaik SJ, Spakman W, Bijl PK, Sluijs A, Langereis CG, Brinkhuis H (2015) A paleolatitude calculator for paleoclimate studies. PLoS One 10:1–21
Walker RG, Plint AG (1992) Wave- and storm-dominated shallow marine systems. In: Walker RG, James NP (eds) Facies models: response to sea level changes. Geological Association of Canada, Newfoundland, pp 219–238
Weiß M (1995) Stratigraphie und Mikrofauna im Kimmeridge SE-Niedersachsens unter besonderer Berücksichtigung der Ostracoden. Clausthaler Geowiss Diss 48:1–274
Wierzbowski A, Atrops F, Grabowski J, Hounslow M, Matyja BA, Olóriz F, Page K, Parent H, Rogov MA, Schweigert G, Villaseñor AB, Wierzbowski H, Wright JK (2016) Towards a consistent Oxfordian/Kimmeridgian global boundary: current state of knowledge. Vol Jur 14:15–50
Williams CJ, Hesselbo SP, Jenkyns HC, Morgans-Bell HS (2001) Quartz silt in mudrocks as a key to sequence stratigraphy (Kimmeridge Clay Formation, Late Jurassic, Wessex Basin, UK). Terra Nova 13:449–455
Wilson JL (1975) Carbonate facies in geologic history. Springer, Berlin
Wings O, Sander PM (2012) The late jurassic vertebrate assemblage of the Langenberg Quarry, Oker, Northern Germany. Â¡ Fundamental 20:281–284
Wright VP, Burchette TP (1996) Shallow-water carbonate environments. In: Reading HG (ed) Sedimentary environments: process, facies and stratigraphy. Blackwell, Oxford, pp 325–394
Ziegler PA (1990) Geological atlas of western and central Europe. Shell internationale petroleum maatschappij BV, Den Haag, p 239